

$\alpha_v\beta_3$ Integrin-Targeting Arg-Gly-Asp (RGD) Peptidomimetics Containing Oligoethylene Glycol (OEG) Spacers

Vincent Rerat,[†] Georges Dive,[‡] Alex A. Cordi,[§] Gordon C. Tucker,[§] Reine Bareille,^{||} Joëlle Amédée,^{||} Laurence Bordenave,^{||,⊥} and Jacqueline Marchand-Brynaert^{*,†}

[†]Unité de Chimie Organique et Médicinale, Université Catholique de Louvain, Bâtiment Lavoisier, Place L. Pasteur 1, 1348 Louvain-la-Neuve, Belgium, [‡]Centre d'Ingénierie des Protéines, Université de Liège, Bâtiment B6, Allée de la Chimie, 4000 Sart-Tilman, Belgium, [§]Institut de Recherches Servier, Rue des Moulineaux 11, 92150 Suresnes, France, ^{||}INSERM, U577, Université Victor Segalen Bordeaux 2, Rue Léo Saignat 146, 33076 Bordeaux Cedex, France, and [⊥]CIC-IT Biomatériaux, INSERM, Pessac, F-33604 France; CHU Bordeaux, Hôpital Xavier Arnoz, Pessac, 33604, France

Received June 9, 2009

RGD peptides are used in biomaterials science for surface modifications with a view to elicit selective cellular responses. Our objective is to replace peptides by small peptidomimetics acting similarly. We designed novel molecules targeting $\alpha_v\beta_3$ integrin and featuring spacer-arms (for surface grafting), which do not disturb the biological activity, from (L) *N*-(3-(trifluoromethyl)benzenesulfonyl) tyrosine used as scaffold. Various Arg-mimics were fixed on the phenol function, and the ortho position was used for the coupling of OEG spacers. All peptidomimetics were active in the nM range in a binding test toward human $\alpha_v\beta_3$ integrin (IC₅₀ = 0.1 to 1.7 nM) and selective versus platelet integrin $\alpha_{IIb}\beta_3$. Selected compounds revealed excellent ability to inhibit bone cells adhesion on vitronectin. Modeling and docking studies were performed for comparing the most active RGD peptidomimetic to cilengitide, i.e., *cyclo*-[RGDfN(Me)V]–. Lastly, the adhesion of endothelial cells on a cultivation support grafted with RGD peptidomimetics was significantly improved.

Introduction

RGD (Arg-Gly-Asp)-based ligands of $\alpha_v\beta_3$ integrin are intensively investigated in topics related to pathology, pharmacology, and materials science. The RGD peptide sequence has been recognized 25 years ago as the cell attachment site in various extracellular matrix (ECM^a) proteins.^{1,2} At the same time, cellular receptors of ECM proteins have been identified and most have been classified in the integrin family. These receptors are heterodimeric transmembrane glycoproteins formed by the association of α and β subunits.^{3–6} They mediate cell adhesion and migration phenomena.

The $\alpha_v\beta_3$ integrin (also called vitronectin receptor) is mainly involved in adhesion of osteoclasts and osteoblasts to bone matrix, migration of vascular smooth muscle cells, angiogenesis

of proliferating endothelium, and tumor invasiveness.^{7–10} Therefore, antagonists of $\alpha_v\beta_3$ receptor, namely RGD cyclic peptides¹¹ and RGD peptidomimetics,^{12,13} are currently developed as potential drugs for the treatment of osteoporosis, restenosis, ocular disease, and cancer.^{14–16} This is exemplified with cilengitide, i.e., *cyclo*-[RGDfN(Me)V]–, actually under clinical trials.¹¹ RGD-based strategies are also considered for the selective delivery of therapeutics and imaging agents to tumor cells.^{17–19} Last, biomaterials for stimulated cell adhesion are prepared by surface modification with RGD molecules.^{20–22}

Controlling the interface between cells and solid substrates is of major concern in tissue engineering and regenerative medicine.²³ In this context, we are interested in the covalent attachment of RGD peptidomimetics on the surface of inert polymer materials such as poly(ethylene terephthalate) (PET), with a view to promote cellular adhesion in the absence of serum or ECM proteins.^{24,25} The development of such a strategy requires peptidomimetic molecules featuring an anchorage arm having a position on the molecular scaffold that does not disturb the biological activity. In this article, we describe the synthesis and the validation of novel RGD peptidomimetics, containing OEG (oligoethylene glycol) spacers, and constructed on the (L)-tyrosine scaffold, for targeting $\alpha_v\beta_3$ integrin. Our aim is the development of molecular devices useful in biomaterials research principally, but also in drug or imaging agent delivery and immunotherapy.^{26,27}

Results and Discussion

Design. The promotion of cellular adhesion on biocompatible polymer substrates is generally achieved either by coating

*To whom correspondence should be addressed. Phone: +32 (0)10 47 27 40. Fax: +32 (0)10 47 41 68. E-mail: jacqueline.marchand@uclouvain.be.

^aAbbreviations: ACN, acetonitrile; Boc, *tert*-butyloxycarbonyl; DMEM, Dulbecco's Modified Eagle Medium; DMF, dimethylformamide; DMSO, dimethylsulfoxide; EC, endothelial cell; ECM, extracellular matrix; EDTA, ethylenediaminetetraacetic acid; EG, ethylene glycol; FCS, fetal calf serum; FtN, phthalimide; GRGDS, glycine-arginine-glycine-aspartic acid-serine; HOP, human osteoprogenitor; HSV, human saphenous vein; IMDM, Iscove Modified Dulbecco's Medium; IC₅₀, half maximal inhibitory concentration; MIDAS, metal ion dependent adhesion site; OEG, oligoethylene glycol; PB, phosphate buffer; PBS, phosphate buffered saline; PET, poly(ethylene terephthalate); PS, polystyrene; PyBop, benzotriazol-1-yl-oxy-tris(dimethylamino)phosphonium hexafluorophosphate; RGD, arginine-glycine-aspartic acid; RHF, restricted Hartree–Fock; TCPS, tissue culture polystyrene; TFA, trifluoroacetic acid; THF, tetrahydrofuran; XPS, X-ray photoelectron spectroscopy.

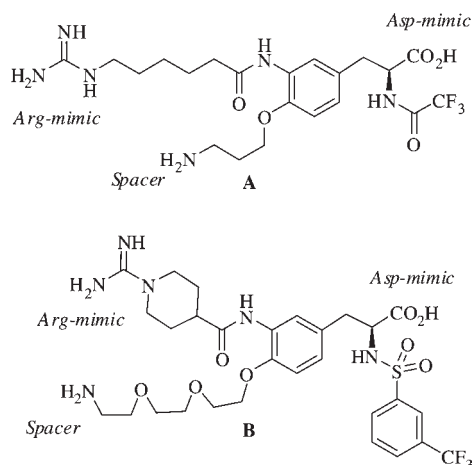


Figure 1. First generation of peptidomimetics based on the (L)-tyrosine scaffold.

the materials with ECM proteins and RGD-containing large peptides²⁰ or by surface derivatization with small (cyclic) RGD peptides^{28,29} and peptidomimetics (i.e., nonpeptide mimics of the RGD sequence constrained in the bioactive conformation). This latter approach is quite underemployed from the literature,²⁵ most probably because it requires expertise and consistent efforts in organic synthesis. As far as inorganic (bio)materials are concerned, the coating of titanium with thiol-terminated RGD peptidomimetics has been reported by Kessler et al.³⁰

Starting from the (L)-tyrosine scaffold,^{31,32} we have already prepared RGD peptidomimetics possessing a free carboxyl function (Asp-mimic) and a guanidino function (Arg-mimic) at a distance of about 13 Å on the one hand, and an anchorage-arm (fixed on aromatic OH) for surface grafting on materials on the other hand.^{33,34} Disappointingly, such molecules, exemplified by **A** and **B** (Figure 1), were poorly active against $\alpha_v\beta_3$, and nonselective versus $\alpha_{IIb}\beta_3$, the integrin receptor expressed on blood platelets.³⁵ Nevertheless, PET membranes surface-derivatized with peptidomimetics **A** and **B** showed improved adhesive properties in CaCo2 cell culture systems.^{24,25} In the course of this preliminary work, evaluation of the parent compound **C** (Figure 2) against $\alpha_v\beta_3$ and $\alpha_{IIb}\beta_3$ integrins gave an unexpected result: this (L)-tyrosine derivative was a modest antagonist of both receptors.

The *O*-aminopropyl chain, initially considered as the spacer-arm, seemed to play the role of the basic function mimicking the Arg residue. We decided thus to investigate a novel family of RGD peptidomimetics derived from (L)-tyrosine in which the relative positions of the Arg-mimic and the spacer-arm were exchanged, as shown in the general structure **D** (Figure 2). The hydrophobic moiety next to the Asp-mimic^{36,37} remained the *meta*-trifluoromethyl-benzenesulfonamide group featuring a useful fluorine-tag for XPS (X-ray photoelectron spectroscopy) analysis of the final biomaterials.²⁵ The basic motifs **R** were chosen among the library of Arg bioisosters usually found in $\alpha_v\beta_3$ antagonists from the recent literature,^{13,38–40} i.e., cyclic amidines, aminopyridines, and tetrahydronaphthyridines. Last, α,ω -functionalized oligoethylene glycols (OEG) were selected as spacer-arms due to the particular properties of OEG molecules well recognized in materials sciences: water solubility, molecular flexibility, stability in biological medium, and antifouling capacity.⁴¹

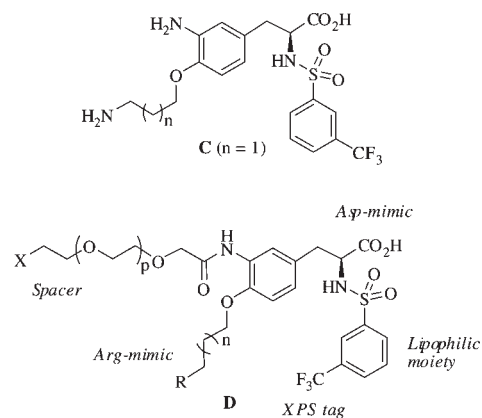
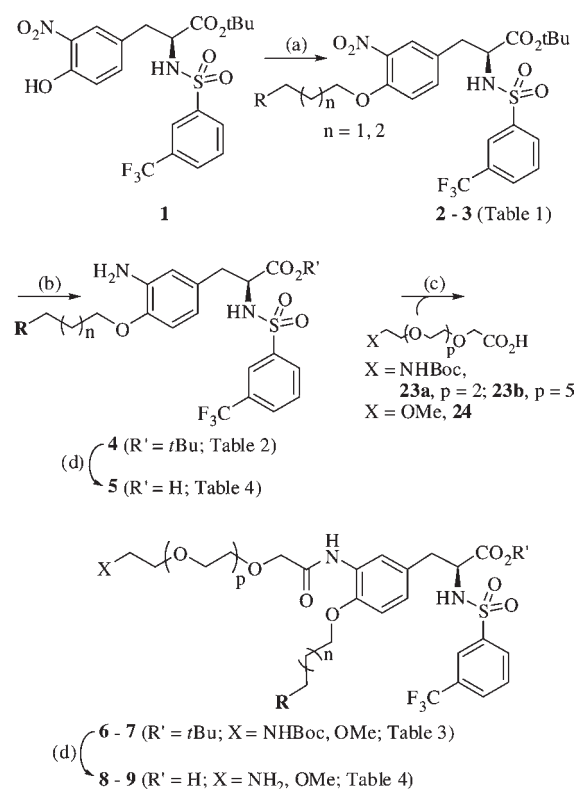


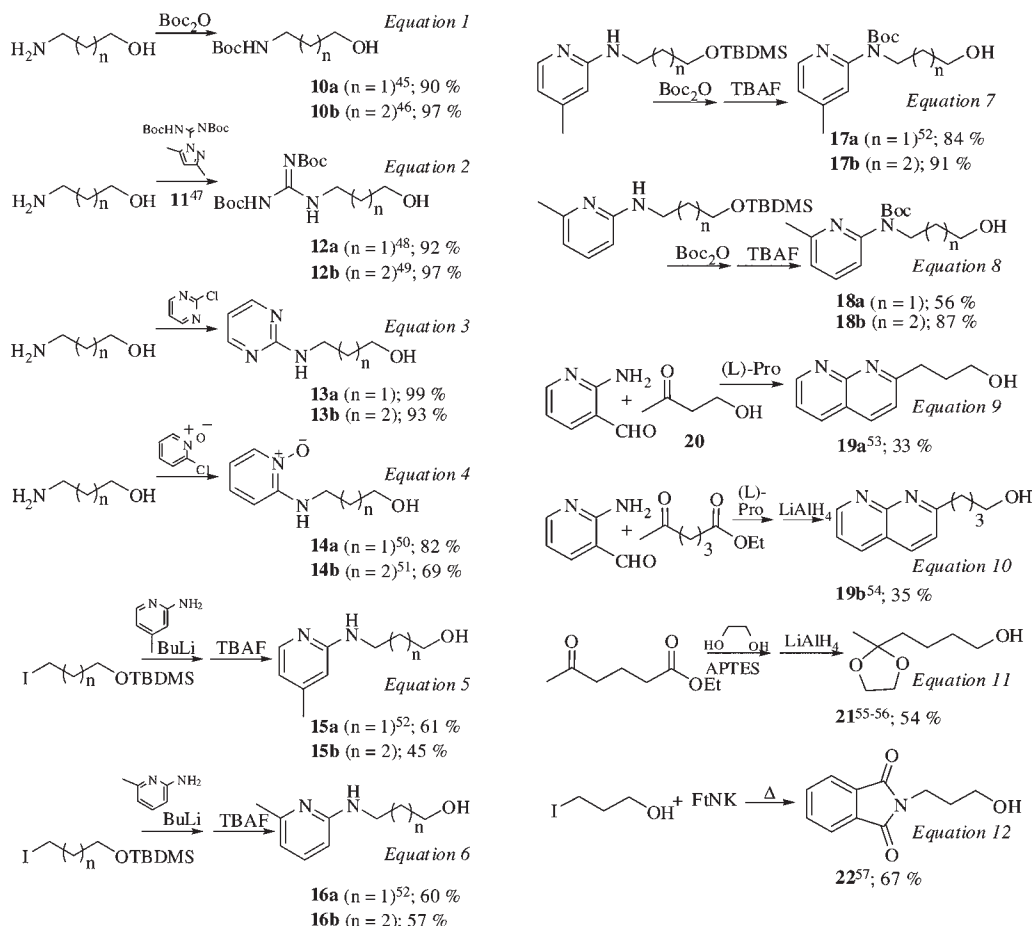
Figure 2. Second generation of peptidomimetics ($n = 1, 2; p = 2, 5; X = NH_2$).

Scheme 1. General Synthesis of Graftable Peptidomimetics^a



^aSteps: (a) Mitsunobu coupling, (b) reduction by hydrogenation, (c) acylation with OEG-spacer, (d) deprotection.

Chemical Synthesis. A convergent strategy was set up for the synthesis of the target-molecules **D** (Figure 2): a key intermediate, namely *t*-butyl 3-(4-hydroxy-3-nitro-phenyl)-2-(*S*)-(3-trifluoromethyl-benzenesulfonylamino)propionate (**1**), was successively equipped with Arg-mimics via a Mitsunobu reaction on the tyrosine-OH and with OEG-spacers via a peptide coupling on the tyrosine-NH₂ obtained by reduction of tyrosine-NO₂ precursors (Scheme 1). The basic motifs were connected by using either a propyl ($n = 1$) or a butyl chain ($n = 2$), in view of adjusting the distance between the acidic and basic moieties to about 12–14 Å.⁴² The length of the spacer was of three ($p = 2$) or six ($p = 5$) ethyleneglycol units, according to a previous study,⁴³ and the terminal function for grafting on materials was a primary amine.

Scheme 2. Synthesis of the Basic Arms as Arg-Mimics (See Supporting Information)

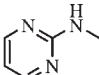
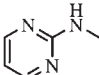
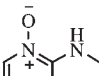
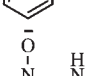
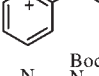
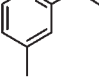
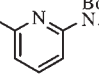
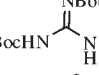
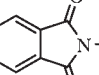
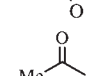
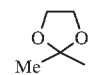
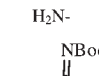
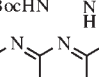
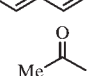
The precursor **1** was already described³⁴ (45% yield in two steps from commercial *t*-butyl tyrosinate; 1 g scale), but as we needed large quantities, a practical synthesis was developed starting from (L)-tyrosine (see Supporting Information). Briefly, *t*-butyl tyrosinate was obtained by transesterification with *t*-butyl acetate in the presence of perchloric acid; sulfonylation was performed with *meta*-trifluoromethylbenzenesulfonyl chloride at 0 °C in THF–DMF mixture (8:1, v/v)⁴⁴ in the presence of solid sodium carbonate; nitration was realized with nitric acid in acetic acid (0.25 M solution) at 16 °C (90% yield on two steps, 20 g scale).

The required ω -functionalized propanols and butanols (with the basic groups) for Mitsunobu coupling to phenol **1** (Scheme 1, step a) were prepared by conventional routes depicted in Scheme 2 (see Supporting Information).^{45–57} *O*-Alkylation of **1** with alcohols **10a,b** (eq 1), **12b** (eq 2), **13a,b** (eq 3), **14a,b** (eq 4), **17b** (eq 7), and **18b** (eq 8), in the presence of diisopropyl azodicarboxylate and triphenylphosphine (THF, 20 °C, 17 h), readily gave compounds **2a–i**, collected in Table 1. The Mitsunobu etherification failed when using alcohols **12a** (eq 2), **15a,b** (eq 5), **16a,b** (eq 6), **17a** (eq 7), **18a** (eq 8), **19a** (eq 9), and **19b** (eq 10) due to the rapid intramolecular cyclization of the activated alcohols or unfavorable steric effects. Therefore, the desired compounds **2–3** were obtained via indirect routes. For instance, in the case of naphthyridine derivatives **3**, the precursors of Friedländer heterocyclization were introduced first, namely 3-acetyl-1-propanol (**20**) and 4-(2-methyl-[1,3] dioxolan-2-yl)butan-1-ol (**21**, eq 11). Thus under Mitsunobu conditions, reaction of **1** with **20** furnished **2k** (entry 11); further condensation with

2-amino-3-pyridine carboxaldehyde ((L)-proline, EtOH, reflux, 24 h)⁵⁴ gave the naphthyridine **3c** (entry 15). Similarly, reaction of **1** with **21** yielded **2l** (entry 12), in which dioxolane deprotection (FeCl₃ on SiO₂, acetone, 20 °C, 2 h)⁵⁸ afforded **3d** (entry 16). Last, Friedländer heterocyclization led to **3e** (entry 17). Etherification of phenol **1** with *N*-phthalimido-3-amino-propan-1-ol (**22**, eq 12) produced **2j** (entry 10); FtN-deprotection (N₂H₄, EtOH, 80 °C, 2 h) gave intermediate **3a** (entry 13), followed by *N*-guanidylation with di-Boc thiourea in the presence of Mukaiyama salt ((BocNH)₂CS, 2-chloro-1-methyl-pyridinium iodide, Et₃N, DMF, 20 °C, 1 h),⁵⁹ which furnished compound **3b** (entry 14).

The series of *O*-alkylated derivatives **2–3** was submitted to hydrogenation for transforming the aromatic NO₂ group into NH₂ function (Scheme 1, step b). The resulting anilines **4** are collected in Table 2. In several cases, the basic substituents could simultaneously suffer reduction giving the required Arg-mimics: catalytic hydrogenation over palladium on charcoal reduced the naphthyridine motif into tetrahydro-naphthyridine (entries 11–12); catalytic hydrogenation in acidic medium reduced the pyrimidine motif into six-membered cyclic amidine together with *t*-butyl ester cleavage (entries 3–4); treatment with ammonium formate and Pd/C catalyst⁶⁰ reduced pyridine oxide into pyridine (entries 5–6). Finally, simultaneous deprotection of *t*-butyl ester and *N*-Boc groups was readily performed by reaction of compounds **4** (except **4c** and **4d**, already deprotected) with trifluoroacetic acid (TFA–CH₂Cl₂ (1:1), 20 °C, 2 h), giving the RGD peptidomimetics **5** listed in Table 4 (entries 1–7 and 12–16) and considered for biological evaluation (see next section).

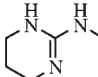
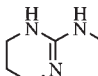
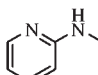
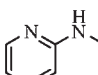
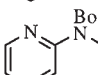
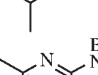
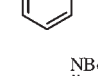
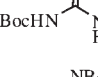
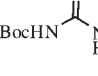
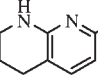
Table 1. *O*-Alkylation of Key Intermediate **1** (Step a)

Entry	R	n	Cmpd	Yield (%) ^a
1	BocNH-	1	2a ³⁴	75
2	BocNH-	2	2b	64
3		1	2c	22
4		2	2d	62
5		1	2e	69
6		2	2f	65
7		2	2g	63
8		2	2h	65
9		2	2i	98
10		1	2j	52
11		1	2k	59
12		2	2l	87
13	H ₂ N-	1	3a	73 ^b
14		1	3b	66 ^c
15		1	3c	49 ^d
16		2	3d	85 ^e
17		2	3e	50 ^f

^a Chromatography. ^b Obtained from **2j** by hydrazinolysis. ^c Obtained from **3a** by guanidylation. ^d Obtained from **2k** by Friedländer reaction. ^e Obtained from **2l** by deprotection. ^f Obtained from **3d** by Friedländer reaction.

Two OEG spacer-arms were prepared following conventional chemistry (see Supporting Information). Briefly, *N*-Boc protected 2-(2-(2-aminoethoxy)ethoxy)ethanol^{61,62} and *t*-butyl 17-hydroxy-3,6,9,12,15-penta-oxaheptadecylcarbamate⁶³ were *O*-alkylated with methyl bromoacetate or ethyl diazoacetate and the resulting esters were saponified to give the corresponding acids **23a** (*p* = 2)⁶⁴ and **23b** (*p* = 5)⁶⁵ used for coupling with aniline derivatives **4** (see Scheme 1, step c). In the presence of benzotriazol-1-yl-oxy-tris-(dimethylamino)phosphonium hexafluorophosphate (PyBOP) as activating agent (Et₃N, DMF, 20 °C, 2 h),

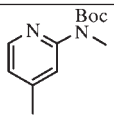
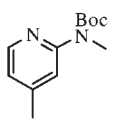
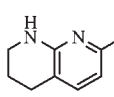
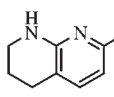
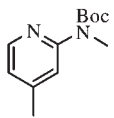
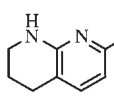
Table 2. Reduction of Nitro Intermediates **2–3** (Step b)

Entry	Reagent	Product				Conditions ^d
		n	R	Cmpd	Yield	
1	2a	1	BocNH-	4a ³⁴	98 ^b	A
2	2b	2	BocNH-	4b	98 ^b	A
3	2c	1		4c ^a	62 ^c	B
4	2d	2		4d ^a	95 ^b	B
5	2e	1		4e	80 ^c	C
6	2f	2		4f	88 ^c	C
7	2g	2		4g	89 ^b	A
8	2h	2		4h	93 ^b	A
9	2i	2		4i	95 ^b	A
10	3b	1		4j	88 ^b	A
11	3c	1		4k	98 ^b	A
12	3e	2		4l	88 ^b	A

^a Simultaneous *t*-butyl ester deprotection is observed (conditions in note^d). ^b After filtration on celite. ^c Isolated product by chromatography. ^d A = Pd/C (10%), H₂ (1 bar), MeOH, 18 h, 20 °C; B = HCl_{aq} (35%)-AcOH (1:9, v/v), Pd/C (10%), H₂ (3 bar), 2 h, 20 °C; C = NH₄⁺HCO₂⁻ (10 equiv), Pd/C (10%), EtOH, 12 h, reflux.

23a and **23b** reacted with **4g** and **4k** (0.9 equiv, DMF, 40 °C, 18 h) to furnish the amides **6a,b** (*p* = 2) and **7a,b** (*p* = 5), respectively (Table 3, entries 1–4). (2-(2-(2-Methoxy-ethoxy)-ethoxy)-ethoxy)-acetic acid (**24**)⁶⁶ (spacer-arm devoid of terminal amine function) was similarly coupled to **4g** and **4k**, giving compounds **6c,d** (entries 5–6). For biological evaluation, the precursors **6–7** were fully deprotected by treatment with TFA (50% in CH₂Cl₂, 20 °C, 2 h) to afford the RGD peptidomimetics **8–9** (Table 4, entries 9–11 and 18–20). Last, the aromatic NH₂ function of intermediates **4g** and **4k** has been acylated (CH₃COCl, Et₃N, CH₂Cl₂, 20 °C, 1 h) and the resulting acetamides (**4m,n**; 62–66%) were deprotected as usual, giving **5m** and **5n** for evaluation (Table 4, entries 8 and 17).

Table 3. Coupling of Spacer-Arms (Step c)

Entry	Reagent	Product					Yield (%)
		n	R	p	X	Cmpd	
1	4g	2		2	NHBoc	6a	37
2	4g	2		5	NHBoc	7a	50
3	4k	1		2	NHBoc	6b	37
4	4k	1		5	NHBoc	7b	33
5	4g	2		2	OMe	6c	61
6	4k	1		2	OMe	6d	45

Biological Evaluation. Our design and synthesis of tyrosine-based RGD peptidomimetics afforded a library of 20 compounds which were evaluated for binding affinity toward human $\alpha_v\beta_3$ integrin by using a competitive assay already described.³⁴ Briefly, the purified integrin was incubated with biotinylated vitronectin (natural ligand) in excess in the presence of various concentrations of the tested compound. The amount of bound natural ligand was measured, indirectly, by incubation with a biotin-directed antibody coupled to alkaline phosphatase and reading at 405 nm of the amount of *p*-nitrophenol liberated by enzymatic hydrolysis of *p*-nitrophenylphosphate. The structurally close platelet integrin $\alpha_{IIb}\beta_3$ was also considered in this study, using a similar colorimetric binding test with fibrinogen as the competitive natural ligand. Results were expressed in IC_{50} values for comparison (Table 4).

Compounds **4c–d** (entries 3–4), **5e–g** (entries 5–7), and **5h–l** (entries 12–16) are all active in the nM range, thus confirming the right position of the Arg-mimics on the tyrosine aromatic core. The selected choice of Arg-mimics was also judicious because the simple NH_2 substituent conferred only modest activity (compounds **5a–b**, entries 1–2). The most active molecules featured either 2-amino-4-methyl-1-pyridin-2-yl or tetrahydro-1-naphthyridin-2-yl substituents (= **R** group) with respectively a butyl ($n = 2$) or a propyl chain ($n = 1$). These RGD peptidomimetics, namely **5g** (entry 7) and **5k** (entry 15), were also highly selective for $\alpha_v\beta_3$ versus $\alpha_{IIb}\beta_3$. They were thus chosen for the anchorage of the spacer-arms.

First of all, their aniline function has been masked to ensure that this function does not make part of the pharmacophore (compounds **5m** and **5n**, entries 8 and 17). Indeed, the acylated peptidomimetics **5m,n** were almost similarly active as their parent compounds but with a drop of selectivity. Fortunately, in both cases, the grafting of spacer-arms with three or six EG units on molecules **5g** and **5k** maintained their excellent activities: IC_{50} values of the graftable peptidomimetics **8a, 9a** (entries 9–10) and **8b, 9b** (entries 18–19) ranged within 0.8–0.9 nM and 0.3–0.7 nM, respectively. Here again, a control experiment consisting in the replacement of the NH_2 spacer end-group with a methoxy group (compounds **8c** and **8d**, entries 11 and 20) showed that this amino function is not involved in the $\alpha_v\beta_3$ recognition process. Thus, all the RGD peptidomimetics containing OEG spacers (**8a, 9a, 8c, 8b, 9b, 8d**) remain active in the nM range against $\alpha_v\beta_3$, but their selectivity versus $\alpha_{IIb}\beta_3$ diminishes, as compared to previously published active molecules designed to be orally bioavailable.⁶⁷

Selected peptidomimetics, namely **5g, 5n**, and **8b**, have been evaluated in solution for their ability to inhibit cellular adhesion in a competitive test versus vitronectin. The assay was realized with HOP (human osteoprogenitor) cells.^{68,69} Cells were preincubated with tested molecules in serum-free medium to saturate the integrin receptors and then seeded on polystyrene (PS) plates coated with vitronectin. Cell attachment was measured by a colorimetric method.⁷⁰ For positive control (100% attachment), cells nonincubated with peptidomimetics were inoculated on the culture plates. GRGDS (Gly-Arg-Gly-Asp-Ser) pentapeptide was used as reference ligand.^{20,71} Results of Figure 3 show that all tested compounds are active to inhibit cell adhesion on PS plates coated with vitronectin. Peptidomimetic **5g** (devoid of spacer-arm) is active against integrins in the μM and nM ranges. In the same experiment, GRGDS was active in the same ranges, but the latter absorbance ratios were significantly superior to those of peptidomimetic **5g** ($p < 0.01$). Peptidomimetic **5m** (devoid of spacer-arm) appears also active in this assay based on living cells as a whole “sensor”, but its corresponding graftable peptidomimetic **8b** (equipped with the spacer-arm) has lost the activity at the nanomolar concentrations. The effect of the spacer-arm has been examined by computational studies.

Modeling Study. A conformational study of selected compounds, namely **4c, 4d, 5e, 5f, 5g, 5h**, and **5k** (see structures in Table 4), has been performed and the critical distances between Arg- and Asp-mimics have been compared to those of cilengitide (*cyclo*-[RGD/N(Me)V]-). All the geometry degrees of freedom were fully optimized at the RHF level using the double- ζ polarized basis set 6-31G(d). For all compounds, at least two conformations could be located: a folded one with a potential π stacking between the two aromatic rings and an extended one which reduces the interactions between the bulky sulfonamide group and the **R** motif of the Arg-mimic. Energy differences (ΔE) between the folded (reference) and the extended conformers are given in Table 5. The extended conformers are generally more stable, except in the case of **4c** and **5k**. The distances between the carbon bearing the carboxyl group and each of the nitrogen atoms of the basic motifs have been determined (Table 5). For the extended conformations, the values ranged within 11–14 Å, as required for an optimal interaction with $\alpha_v\beta_3$ receptor. Our molecules compare with the cyclic peptide cilengitide for which the bioactive conformation is known from X-ray data.⁷² Their extended conformations are in good agreement with the three-point pharmacophore

Table 4. RGD Peptidomimetics for Biological Evaluation

Entry	Cmpd	R	n	[Spacer]	IC ₅₀ (nM) ^a		
					α _v β ₃	α _{IIb} β ₃	S ^b
1	5a ⁷⁴	NH ₂	1	NH ₂	138	429	3.1 ^c
2	5b	NH ₂	2	NH ₂	428	154	0.35 ^c
3	4c		1	NH ₂	3.9	21.3	5.5
4	4d		2	NH ₂	0.8	101	126
5	5e		1	NH ₂	1.2	36	30
6	5f		2	NH ₂	1.4	70	50
7	5g		2	NH ₂	0.6	106	177
8	5m		2	NHCOMe	0.7	38	54
9	8a		2	HNOC-CH ₂ -O-(CH ₂) ₂ -O-CH ₂ -NH ₂	0.9	28	31
10	9a		2	HNOC-CH ₂ -O-(CH ₂) ₅ -O-CH ₂ -NH ₂	0.8	38	47
11	8c		2	HNOC-CH ₂ -O-(CH ₂) ₂ -O-CH ₂ -OMe	0.5	61	122
12	5h		2	NH ₂	1.7	121	71
13	5i		1	NH ₂	7.6	27	3.5
14	5j		2	NH ₂	1.7	7.3	4.3
15	5k		1	NH ₂	0.1	140.6	1406
16	5l		2	NH ₂	1.1	355	323
17	5n		1	NHCOMe	0.6	71	118
18	8b		1	HNOC-CH ₂ -O-(CH ₂) ₂ -O-CH ₂ -NH ₂	0.3	25	83
19	9b		1	HNOC-CH ₂ -O-(CH ₂) ₅ -O-CH ₂ -NH ₂	0.7	51	73
20	8d		1	HNOC-CH ₂ -O-(CH ₂) ₂ -O-CH ₂ -OMe	0.3	20	67

^a Mean of at least two experiments. ^b Selectivity (S) = $IC_{50} \alpha_{IIb}\beta_3 / IC_{50} \alpha_v\beta_3$. ^c For comparison, GRGDS pentapeptide IC_{50} values are 750 nM ($\alpha_v\beta_3$) and 120 nM ($\alpha_{IIb}\beta_3$).⁷¹

proposed by Moitessier et al. on the basis of geometric considerations.⁷³

Because of the size of the systems, the graftable peptidomimetics **8a** and **8b** (see structures in Table 4) were studied in MINI1 basis. Two accessible extended conformations were found, referred to as Exten 1 (reference) and Exten 2 (Figure 4). Exten 1 features the spacer-arm perpendicularly to the tyrosine scaffold, while Exten 2 is stabilized by a hydrogen bonding between arylamide NH and arylether O due to a rotation of the spacer-arm. As shown in Table 6, the presence of a spacer-arm did not disturb the characteristic distances between Arg- and Asp-mimics.

The conformer Exten 1 of **8b** was superimposed on the crystallographic structure of *cyclo*-[RGD/N(Me)V]— extracted from its complex with the receptor. This shows a good fitting of

the Arg- and Asp-mimics and the orientation of the space-arm alongside the V residue of cilengtide (Figure 5), thus well positioned for pointing out the receptor recognition pocket.

To further confirm the design of our peptidomimetic, **5k** (extended conformer) was docked in the active site of $\alpha_v\beta_3$, obtained from the X-ray crystal structure of the extracellular segment of the $\alpha_v\beta_3$ integrin complexed with cilengtide.^{74,75} The goodness of fit appeared very interesting as the naphthyridinyl part can be in direct electrostatic interaction with the Asp218 residue (from the α_v subunit) and the carboxylic head is charge paired with the Arg214 residue (from the β_3 subunit) and Mn^{2+} ion (from the metal ion dependent adhesion site, MIDAS) (Figure 6). As the molecule **5k** is rather flexible, a complementary optimization has been performed starting from several conformations which can be fitted in the active site. Remarkably,

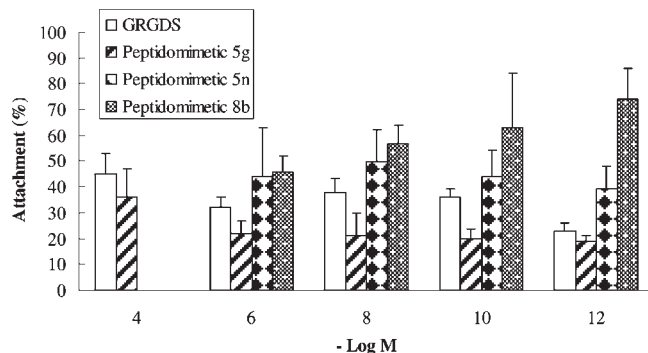


Figure 3. Inhibition of HOP cell attachment on vitronectin by GRGDS peptide and the synthesized peptidomimetics.

Table 5. Conformational Study of Peptidomimetics without Spacer-Arm

entry	compd (Table 4)	ΔE^c (kcal·mol ⁻¹)	distances C-CO ₂ H/N (Å) ^a	
			folded conformation	extended conformation
1	4c	+0.532	7.09; 8.17; 9.12	10.92; 12.05; 13.18
2	4d	-2.239	10.12; 10.89; 12.05	12.03; 13.77; 14.23
3	5e	-0.054	6.97; 7.71	10.93; 13.11
4	5f	-1.413	9.00; 10.56	12.03; 14.13
5	5g	-1.195	8.89; 10.42	12.03; 14.13
6	5h	-1.678	10.07; 11.81	12.03; 14.13
7	5k	+1.563	6.90; 7.14	11.96; 14.16
8	cilengitide ^b		10.99; 11.62; 12.57	

^aDistances between C (bearing the carboxyl group) and each N atom of the Arg-mimic. ^bStructure from X-ray data of the complex with the receptor. ^c $\Delta E = E_{\text{extended}} - E_{\text{folded}}$ (RHF/6-31G(d)).

Table 6. Conformational Study of Graftable Peptidomimetics

entry	compd (Table 4)	Distances C-CO ₂ H / N (Å) ^a		ΔE^b (kcal·mol ⁻¹)
		Exten 1	Exten 2	
1	8a	12.25; 14.45	12.22; 14.41	7.41
2	8b	11.64; 13.50	11.50; 13.23	7.31

^aDistances between C (bearing the carboxyl group) and each N atom of the Arg-mimic. ^b $\Delta E = \Delta E_{\text{exten1}} - \Delta E_{\text{exten2}}$ (MINI-1').

the reoptimized minima remained in the local conformation without significant modifications of the dihedral angles defining the principal skeleton in an energetic range less than 3 kcal·mol⁻¹. The main difference is only the rotation of the phenyl-sulfonamide fragment (Figure 7). In the same way, with a view to validate our docking simulation, *cyclo*-[RGD/N(Me)V]— was optimized at the RHF/6-31G(d) level. Again, several conformations could be located and the observed X-ray conformation remained a local minimum when reoptimized (see Supporting Information).

Application to a Cell Culture System. A poly(ethylene terephthalate) (PET) track-etched membrane currently used as cell culture support^{24,25} was derivatized with peptidomimetic molecules **8b**, **9a**, **9b**, and GRGDS peptide by surface covalent grafting. The native membrane was activated by a wet chemistry treatment with trifluorotriazine⁷⁶ and then incubated with the adhesive molecules to furnish the supports named PET-g-**8b**, PET-g-**9a**, PET-g-**9b**, and PET-g-RGD, respectively. The rates of surface functionalization were determined by X-ray photoelectron spectroscopy (XPS)⁴³ and the recorded percentages of grafting converted into pmol/cm² of apparent surface for comparing the samples.

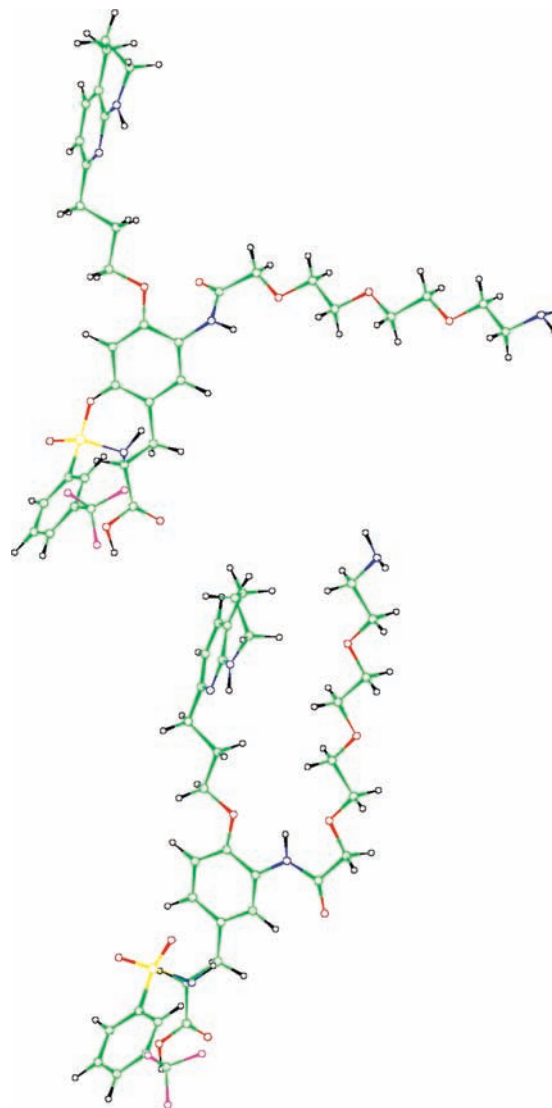


Figure 4. Two conformers of **8b** obtained by calculation in MINI-1' basis.

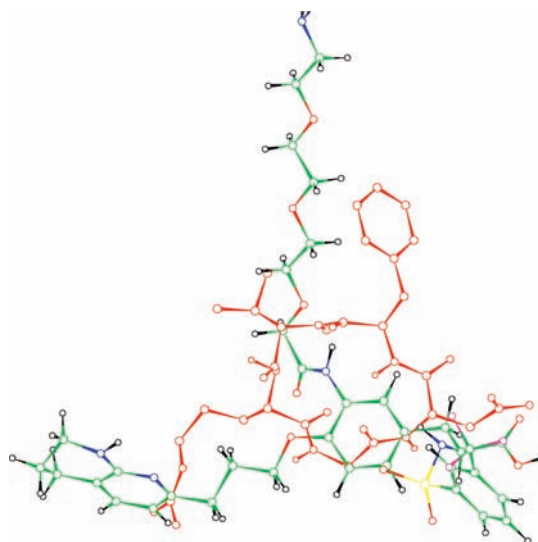


Figure 5. Superimposition of the conformer exten1 of **8b** and cilengitide.

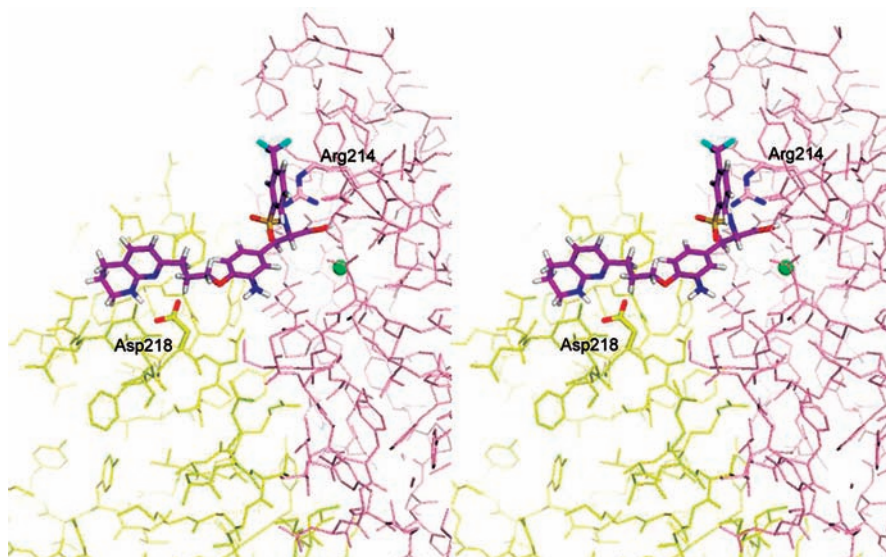


Figure 6. Docking of **5k** in the active site of integrin $\alpha\beta 3$. The α and β subunits of integrin are colored yellow and pink, respectively. **5k** is colored purple. Oxygen atoms are red, nitrogen atoms are blue, hydrogen atoms are white, and fluorine atoms are cyan. The Mn^{+2} ion is shown as a green sphere.

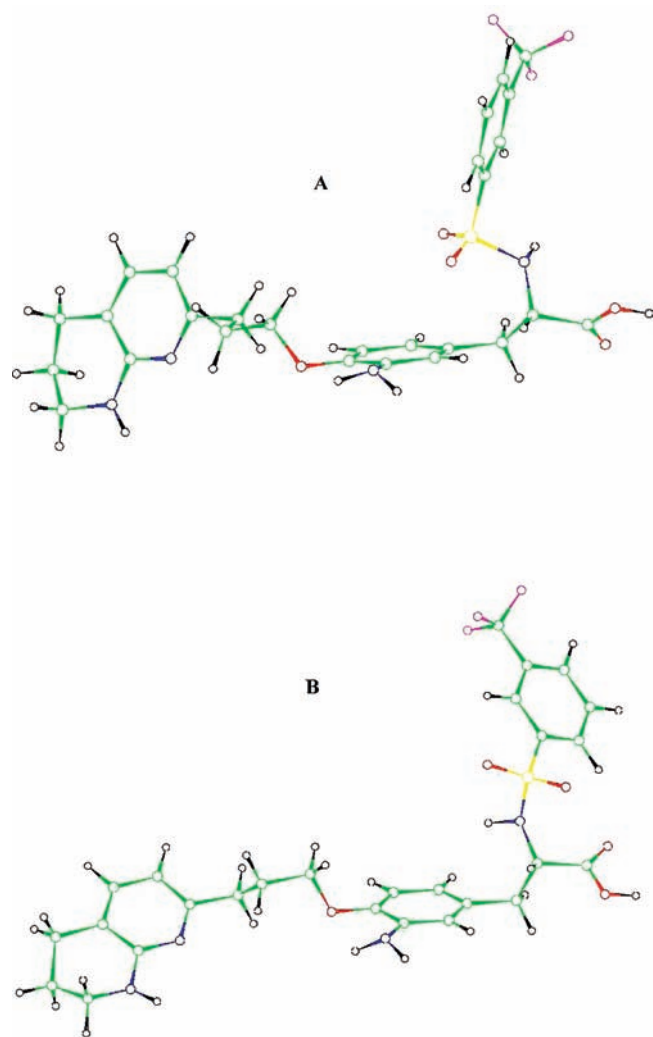


Figure 7. Conformer **5k** obtained from docking (A) and reoptimized (B).

The modified surfaces were investigated with human endothelial cells (EC) isolated from human saphenous veins

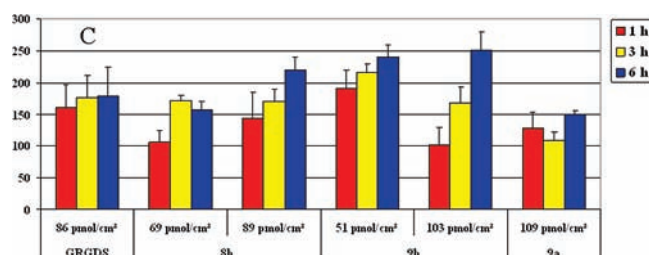


Figure 8. HSVEC attachment on surface-modified PET substrates.

(HSV) collected after surgical coronary bypass. Cells were cultured under specific conditions and used in the fourth passage.⁷⁷ Cells were seeded on native PET membrane and surface modified supports, in the absence of serum, at the density of 50000 HSVECs per cm² for 1, 3, and 6 h. Thereafter, nonadherent cells were removed by washings and adherent cells assayed by a quantitative colorimetric test.⁷⁰

Results presented in Figure 8 are expressed in percentages of absorbance related to untreated PET, set at 100%. This blank sample (native PET) is systematically included in each test run for comparing the treated PET samples. The PET-*g*-RGD support is considered as the adhesive control (C) for evaluating the effects of the nonpeptide mimics. The naphthyridin peptidomimetic **8b** equipped with a three EG-units spacer showed a significant effect of surface concentration increase (from 69 to 89 pmol/cm²) on cell attachment at 6 h ($p < 0.001$, see columns 2 and 3). For similar surface densities, the naphthyridin peptidomimetic **9b** featuring a longer spacer-arm (i.e., six EG-units) was significantly more active at 1, 3, and 6 h for promoting HSVECs adhesion ($p < 0.004$, see columns 2 and 4). But increasing the surface density of **9b** did not improve further the performances at 6 h (from 51 to 103 pmol/cm², see columns 4 and 5). Last, for similar surface densities (103–109 pmol/cm²) and the same length of the spacer-arm (six EG-units), the 4-methyl-2-amino-pyridine peptidomimetic **9a** was less efficient than the naphthyridin one **9b** at 3 and 6 h (see columns 5 and 6). Regarding the control surface (column 1), the PET-*g*-**9b** support with a functionalization rate of about 50 pmol/cm² (column 4) appears of particular interest for further studies. This novel substrate allows an increase

of cellular attachment of 200–250% in a serum-free culture medium, in comparison with the commercial (native) PET membrane, while the performance of PET-*g*-RGD (about 85 pmol/cm²) is lower (150–180%).

Conclusion

The idea that RGD-peptidomimetic molecules could be equipped with a spacer-arm without disturbing their capacity to bind the $\alpha_v\beta_3$ integrin has been successfully exploited in the case of ligands based on the tyrosine scaffold. This scaffold was initially considered by the Merck group for the research of platelet receptor $\alpha_{IIb}\beta_3$ antagonists,⁷⁸ giving tirofiban as cardiovascular drug, and more recently used by Kessler et al. for the design of selective $\alpha_5\beta_1$ ligands,^{42,52} potentially useful in the field of antiangiogenic cancer therapy. Both receptors, $\alpha_{IIb}\beta_3$ and $\alpha_5\beta_1$ feature high sequence similarity with $\alpha_v\beta_3$ integrin.

Practically, we have introduced the spacer-arm on the tyrosine aromatic ring thanks to a simple sequence of reactions involving nitration/reduction/acetylation. It is worth noting that this position of functionalization is unusual. Other studies devoted to bifunctional ligands targeting tumor cells, in the fields of drug delivery and imaging contrast agents, made use of the lipophilic moiety (i.e., the sulfonamide group of piperazine-based RGD peptidomimetics) to couple the spacer.^{79–81}

All the synthesized compounds showed natural ligand displacement competence in the nM range for $\alpha_v\beta_3$, with a variable selectivity versus $\alpha_{IIb}\beta_3$ ($S = 1.4 \cdot 10^3$ for **5k** and $0.83 \cdot 10^2$ for **8b**; $S = 1.8 \cdot 10^2$ for **5g** and $0.3 \cdot 10^2$ for **8a**, see Table 4). The drop of selectivity related to the presence of OEG spacers could not be presently explained. Although $\alpha_v\beta_3/\alpha_{IIb}\beta_3$ selectivity is an important parameter for therapeutic applications, this aspect is not a limiting factor when peptidomimetics are devoted to ex vivo surface modification of biomaterials. Similarly to the reference peptide GRGDS, peptidomimetics **5** and **8** were able to inhibit HOP cell adhesion on a vitronectin-coated support.

Computational studies have confirmed the good fitting of our graftable RGD-peptidomimetics into the target receptor and the possible positioning of the spacer-arm outside the binding site. This is exactly the requirement for the development of molecules **8a,b** and **9a,b** in the field cell adhesive materials with a view of endothelialisation of vascular grafts.⁷⁷ Preliminary results of HSV (human saphenous vein) cell adhesion on poly(ethylene terephthalate) (PET) membranes grafted with peptidomimetics demonstrated the good performance of one substrate, namely PET-*g*-**9b**. Further works are in progress for studying EC proliferation and response under physiological shear stress conditions in flow chambers.

Experimental Section

Chemistry. Reagents were purchased from Aldrich or Acros Organics and used as received. Anhydrous solvents were purchased from Fluka. Reactions needing anhydrous conditions were performed in flame-dried glassware, placed under an argon atmosphere. ¹H and ¹³C NMR spectra were recorded on Bruker 300 Ultra Shield and Bruker AM 500 spectrometers, using deuterated solvents from Rocc SA (Belgium) and TMS (tetramethylsilane) as internal standard. Patterns are designed as s (singlet), br s (broad singlet), d (doublet), dd (doublet of doublet), t (triplet), q (quartet), m (multiplet). Coupling constants (*J*) are given in hertz (Hz). IR spectra were recorded on a

Shimadzu FTIR 8400S equipment; products were deposited as thin films on NaCl crystal. Low resolution mass spectra were obtained with a TSQ 7000 spectrometer from Finnigan in CI (chemical ionization) mode and with a LCQ or quantum spectrometer from Finnigan in ESI (electrospray ionization) mode at 70 eV and APCI (atmospheric pressure chemical ionization) mode at 100 eV. High resolution mass spectra (HRMS) were recorded at the University of Mons-Hainaut, laboratory of professor R. Flammang. Melting points were measured on a Buchi B-540 apparatus calibrated with benzoic acid and are uncorrected. Rotations were measured on a Perkin-Elmer 241 MC apparatus using sodium D ray, at 25 °C; concentrations are given in g/100 mL. Elemental analyses were made in the Christopher Ingold laboratories (Department of Chemistry, Imperial College, London). Analytical thin layer chromatography (TLC) was carried out on Merck TLC plates coated with silica gel 60 F₂₅₄ (0.25 mm layer thickness); visualization was carried out using either a UV lamp (254 nm), or KMnO₄, phosphomolybdic acid (10% in ethanol), and ninhydrin (10% in ethanol) as indicators. Flash chromatography was performed with Merck 60 silica gel (230–400 mesh ASTM). Solvent mixtures used for TLC and flash chromatography are reported in v/v total. Lyophilization of aqueous solutions was realized on a Alpha 2–4LD-plus equipment from Christ (Osterode, Germany). The purity of tested compounds (at least 95%) was established by analytical HPLC using a Waters (Belgium) equipment (Waters 600 pump, Waters 600 multi-solvent controller, 996 photodiode array detector, injection system of Mistral, Spark Holland and EMPOWER software), and a chiralcel OD-H column (5 μm) from Daicel Chemical Industries (Illkirch, France) of 250 mm × 4.6 mm (internal diameter). Elution was made with a mixture of hexane (HPLC grade Chromasolv, Sigma-Aldrich) and *i*-propyl alcohol (HPLC grade HiPerSolv Chromanorm, VWR), in linear gradient mode (from Hex/*i*-PrOH 75:25 to Hex/*i*-PrOH 40:60 over 30 min) at a flow rate of 1 mL/min and temperature of 22 °C (detection at 254 nm).

Selected compounds are fully described below. For the others, namely **2b**, **2c**, **2d**, **2e**, **2f**, **2h**, **2i**, **2j**, **2l**, **3a**, **3b**, **3d**, **3e**, **4b**, **4c**, **4d**, **4e**, **4f**, **4h**, **4i**, **4j**, **4l**, **6c**, **6d**, **5b**, **5e**, **5f**, **5h**, **5i**, **5j**, and **5k**, see Supporting Information.

General Procedure for Coupling Alcohols to Key Intermediate 1 (Table 1). Tyrosine scaffold **1** (0.5 g, 1.02 mmol, 1 equiv) and alcohol (from Scheme 2, 1.12 mmol, 1.1 equiv) were dissolved in dry THF (4 mL) under argon atmosphere, and cooled at 0 °C. Ph₃P (0.4 g, 1.53 mmol, 1.5 equiv) and then DIAD (0.3 mL, 1.43 mmol, 1.4 equiv) were added dropwise. The stirred mixture was allowed to reach slowly room temperature and further left for 1–12 h at 20 °C. Concentration under vacuum and flash chromatography on silica gel gave the coupled product **2** of Table 1.

(S)-*t*-Butyl 3-(4-(4-(*t*-Butoxycarbonyl(4-methylpyridin-2-yl)-amino)butoxy)-3-nitrophenyl)-2-(3-(trifluoromethyl)phenylsulfonamido)propanoate (2g). The title compound was obtained from **17b** (0.250 g, 0.89 mmol) as a pale-yellow oil (0.424 g, 63%). *R*_f (nHex/EtOAc 6:4) = 0.6. IR 2978, 1701, 1533, 1327, 1161 cm⁻¹. ¹H NMR (500 MHz, CDCl₃) δ 1.26 (s, 9H), 1.5 (s, 9H), 1.83 (m, 4H), 2.33 (s, 3H), 2.99 (m, 1H), 3.07 (m, 1H), 3.98 (t, *J* = 6.4 Hz, 2H), 4.06 (m, 3H), 5.26 (d, *J* = 6.5 Hz, SO₂NH, 1H), 6.84 (d, *J* = 5.1 Hz, 1H), 6.93 (d, *J* = 8.6 Hz, 1H), 7.35 (dd, *J* = 8.6, 2.2 Hz, 1H), 7.4 (s, 1H), 7.55 (s, 1H), 7.61 (t, *J* = 7.8 Hz, 1H), 7.79 (d, *J* = 7.8 Hz, 1H), 7.96 (d, *J* = 7.9 Hz, 1H), 8.04 (s, 1H), 8.21 (d, *J* = 5.1 Hz, 1H). ¹³C NMR (125 MHz, CDCl₃) δ 21, 25.25, 26.25, 27.55, 28.18, 37.98, 46.15, 56.68, 69.23, 80.8, 83.63, 114.38, 120.57, 120.88, 124.08, 124.7 (CF₃), 126.41, 127.18, 129.24, 129.76, 130.34, 131.55, 135.44, 139.08, 140.95, 147.18, 148.14, 151.54, 154.18, 154.46, 169.23. MS (APCI) *m/z* 697, 641. HRMS C₃₅H₄₃F₃N₄O₆S calcd for [M + Na]⁺, 775.2601; found, 775.2628.

(S)-*t*-Butyl 3-(3-Nitro-4-(4-oxo-pentyl)oxy)phenyl)-2-(3-(trifluoromethyl)phenylsulfonamido)propanoate (2k). The title compound was

obtained from **20** (0.082 mL, 0.861 mmol) as a pale-yellow oil (0.277 g, 59%). R_f (ether/*n*Hex 85:15) = 0.46. IR 2978, 1716, 1531, 1327, 1163 cm^{-1} . ^1H NMR (300 MHz, CDCl_3) δ 1.27 (s, 9 H), 2.09 (m, 2 H), 2.19 (s, 3 H), 2.73 (t, $J = 6.8$ Hz, 2 H), 2.99 (m, 1 H), 3.07 (m, 1 H), 4.06 (m, 3 H), 5.45 (d, $J = 8.9$ Hz, SO_2NH , 1 H), 6.96 (d, $J = 8.6$ Hz, 1 H), 7.37 (dd, $J = 8.6, 2.2$ Hz, 1 H), 7.6 (d, $J = 2.2$ Hz, 1 H), 7.63 (t, $J = 7.8$ Hz, 1 H), 7.8 (d, $J = 7.8$ Hz, 1 H), 7.98 (d, $J = 7.8$ Hz, 1 H), 8.04 (s, 1 H). ^{13}C NMR (75 MHz, CDCl_3) δ 23.06, 27.86, 30.29, 38.24, 39.45, 57.08, 68.47, 84, 114.73, 124.35, 126.69, 127.68, 129.66, 130.17, 130.68, 131.55, 135.81, 139.11, 141.07, 151.73, 169.38, 208.47, (CF_3 not visible). MS (APCI) m/z 573 $[\text{M} - \text{H}]^-$, 517. HRMS $\text{C}_{25}\text{H}_{29}\text{F}_3\text{N}_2\text{O}_8\text{S}$ calcd for $[\text{M} + \text{Na}]^+$, 597.1494; found, 597.1481.

(S)-*t*-Butyl 3-(4-(3-[1,8]Naphthyridin-2-yl-propoxy)-3-nitrophenyl)-2-(3-(trifluoromethyl)phenylsulfonamido)propanoate (3c). A solution of 2-amino-3-pyridin-carboxaldehyde (0.064 g, 0.517 mmol), precursor **2k** (0.270 g, 0.470 mmol) and (*L*)-proline (0.027 g, 0.235 mmol) in EtOH (5 mL) was refluxed for 48 h under Ar atmosphere. After concentration under vacuum, the residue was purified by chromatography to afford the title compound (0.167 g, 49%) as a white solid. R_f (DCM/*i*-PrOH 98:2) = 0.4. mp = 143–144 °C. IR 1731, 1610, 1533, 1327, 1161 cm^{-1} . ^1H NMR (500 MHz, CDCl_3) δ 1.26 (s, 9 H), 2.51 (quint, $J = 6.3$ Hz, 2 H), 2.97 (m, 1 H), 3.05 (m, 1 H), 3.3 (t, $J = 6.3$ Hz, 2 H), 4.06 (m, 1 H), 4.2 (t, $J = 6.3$ Hz, 2 H), 5.38 (d, $J = 9$ Hz, SO_2NH , 1 H), 6.97 (d, $J = 8.6$ Hz, 1 H), 7.33 (dd, $J = 8.6, 2.2$ Hz, 1 H), 7.46 (d, $J = 8.4$ Hz, 1 H), 7.46 (dd, $J = 7.9, 4.3$ Hz, 1 H), 7.57 (d, $J = 2.2$ Hz, 1 H), 7.6 (t, $J = 7.8$ Hz, 1 H), 7.77 (d, $J = 7.8$ Hz, 1 H), 7.96 (d, $J = 7.8$ Hz, 1 H), 8.03 (s, 1 H), 8.11 (d, $J = 8.4$ Hz, 1 H), 8.17 (dd, $J = 7.9, 2$ Hz, 1 H), 9.08 (dd, $J = 4.3, 2$ Hz, 1 H). ^{13}C NMR (125 MHz, CDCl_3) δ 27.45, 27.55, 34.58, 37.95, 56.73, 68.52, 83.69, 114.49, 121.06, 121.44, 123.02, 124.07, 126.33, 127.12, 129.3, 129.81, 130.34, 131.55, 135.38, 136.74, 137.03, 139.07, 140.78, 151.55, 153.2, 155.83, 165.18, 169.03, (CF_3 not visible). MS (ESI) m/z 1318 $[\text{M} - \text{H}]^- \times 2$, 659 $[\text{M} - \text{H}]^-$, 209. HRMS $\text{C}_{31}\text{H}_{31}\text{F}_3\text{N}_4\text{O}_7\text{S}$ calcd for $[\text{M} + \text{H}]^+$, 661.1944; found, 661.1949.

General Procedure for Reduction of 2–3 (Table 2). **Method A.** A solution of **2** or **3** in MeOH or EtOH (0.1 mmol/3 mL) containing Pd/C (10%) as catalyst (0.01 g/0.1 mmol product **2** or **3**) was placed under H_2 atmosphere (1 atm) and stirred for 18 h at 20 °C. The mixture was filtered over a short celite pad, using MeOH (EtOH); filtrate concentration under vacuum gave quantitatively crude **4**.

Method B. A solution of **2** (0.2 mmol) in HOAc (5 mL) and 37% HCl_{aq} (0.5 mL), containing Pd/C (10%) as catalyst (0.1 g) was introduced in a Parr flask. The mixture was hydrogenated (Parr apparatus) for 2 h at 20 °C, under a pressure of 45 psi. The mixture was filtered on a celite pad, using MeOH– H_2O . Concentration under vacuum and chromatography gave crude **4**, recovered by lyophilization.

Method C. A solution of **2** (0.5 mmol) and ammonium formate (5 mmol) in EtOH (5 mL), containing Pd/C (10%) as catalyst (0.05 g), was refluxed for 12 h under Ar atmosphere and vigorous stirring. The mixture was filtered on a celite pad, using EtOH. After concentration, the residue was dissolved in EtOAc (10 mL), washed with brine (2 \times 5 mL), and dried (MgSO_4). Solvent evaporation gave crude compound **4**.

(S)-*t*-Butyl 3-(3-Amino-4-(4-(*t*-butoxycarbonyl(4-methylpyridin-2-yl)amino)butoxy)phenyl)-2-(3-(trifluoromethyl)phenylsulfonamido)propanoate (4g). The title compound was obtained from **2g** (0.420 g, 0.560 mmol), according to method A, as a pale-yellow oil (0.361 g, 89%). R_f (ether/EtOAc 9:1) = 0.9. $[\alpha]_D^{20} - 11$ ($c = 1.3$, CHCl_3). IR 2975, 1703, 1325, 1159 cm^{-1} . ^1H NMR (500 MHz, CDCl_3) δ 1.26 (s, 9 H), 1.49 (s, 9 H), 1.79 (m, 4 H), 2.33 (s, 3 H), 2.87 (m, 2 H), 3.71 (br s, NH_2 , 2 H), 3.93 (t, $J = 6$ Hz, 2 H), 3.99 (t, $J = 7$ Hz, 2 H), 4.06 (m, 1 H), 5.16 (d, $J = 8.9$ Hz, SO_2NH , 1 H), 6.39 (dd, $J = 8, 2.1$ Hz, 1 H), 6.43 (d, $J = 2.1$ Hz, 1 H), 6.57 (d, $J = 8.2$ Hz, 1 H), 6.84 (d, $J = 5.3$ Hz, 1 H), 7.39 (s, 1 H), 7.57 (t, $J = 7.8$ Hz, 1 H), 7.75 (d, $J = 7.8$ Hz, 1 H), 7.91 (d, $J = 7.8$ Hz, 1 H), 8.05 (s, 1 H), 8.21 (d, $J = 5.3$ Hz, 1 H). ^{13}C NMR (125 MHz, CDCl_3) δ

21, 25.44, 26.56, 27.57, 28.22, 38.76, 46.42, 56.96, 67.86, 80.64, 82.6, 111.07, 115.78, 119.16, 119.51, 120.99, 124.1, 124.7 (CF_3), 127.07, 129.04, 129.6, 130.37, 131.35, 136.12, 141.13, 145.72, 147.18, 148.14, 154.18, 154.46, 169.53. MS (APCI) m/z 721 $[\text{M} - \text{H}]^-$, 621, 209. HRMS $\text{C}_{35}\text{H}_{45}\text{F}_3\text{N}_4\text{O}_7\text{S}$ calcd for $[\text{M} + \text{H}]^+$, 723.3039; found, 723.3057. Anal. calcd (%) C, 58.17; H, 6.23; N, 7.76; S, 4.45. Found C, 58.13; H, 6.37; N, 7.75; S, 4.98.

(S)-*t*-Butyl 3-(3-Amino-4-(3-(5,6,7,8-tetrahydro-1,8-naphthyridin-2-yl)propoxy)phenyl)-2-(3-(trifluoromethyl)phenylsulfonamido)propanoate (4k). The title compound was obtained from **3c** (0.150 g, 0.227 mmol), according to method A, as a pale-brown foam (0.143 g, 98%). R_f (EtOAc/acetone 8:2) = 0.2. $[\alpha]_D^{20} - 11$ ($c = 1$, CHCl_3). IR 2955, 1731, 1651, 1518, 1327, 1159 cm^{-1} . ^1H NMR (500 MHz, CDCl_3) δ 1.21 (s, 9 H), 1.9 (m, 2 H), 2.25 (m, 2 H), 2.68 (br s, NH_2 , 2 H), 2.71 (t, $J = 6.1$ Hz, 2 H), 2.85 (m, 2 H), 2.91 (t, $J = 7.4$ Hz, 2 H), 3.47 (m, 2 H), 3.93 (t, $J = 5.8$ Hz, 2 H), 4.02 (m, 1 H), 5.5 (m, SO_2NH , 1 H), 6.35 (m, 2 H), 6.43 (s, 1 H), 6.57 (d, $J = 8.4$ Hz, 1 H), 7.26 (d, $J = 7.3$ Hz, 1 H), 7.56 (t, $J = 7.8$ Hz, 1 H), 7.73 (d, $J = 7.8$ Hz, 1 H), 7.9 (d, $J = 7.8$ Hz, 1 H), 8.01 (br s, NH, 1 H), 8.1 (br s, 1 H). ^{13}C NMR (125 MHz, CDCl_3) δ 19.44, 25.42, 27.56, 28.51, 30.17, 38.59, 40.91, 57.16, 66.39, 82.55, 109.98, 111.03, 115.92, 117.92, 118.92, 124, 124.7 (CF_3), 127.5, 129, 129.64, 130.38, 131.35, 136.26, 139.96, 141.25, 145.33, 148.69, 152.46, 169.71. MS (ESI) m/z 635 $[\text{M} + \text{H}]^+$, 579. HRMS $\text{C}_{31}\text{H}_{37}\text{F}_3\text{N}_4\text{O}_8\text{S}$ calcd for $[\text{M} + \text{H}]^+$, 635.2515; found, 635.2525. Anal. Calcd for $\text{M} \cdot 0.5\text{H}_2\text{O}$ (%) C, 57.85; H, 5.90. Found C, 58.02; H, 5.82.

General Procedure for Acylation of 4. Precursor **4** (0.1 mmol) dissolved in DCM (2 mL) was treated successively with Et_3N (0.11 mmol) and acetyl chloride (0.11 mmol) at 0 °C under Ar atmosphere. The mixture was stirred for 15 min at 0 °C and 1 h at 20 °C. Dilution with EtOAc, washing with water, drying (MgSO_4) and chromatography gave the acetanilide.

(S)-*t*-Butyl 3-(3-Acetamido-4-(4-(*t*-butoxycarbonyl(4-methylpyridin-2-yl)amino)butoxy)phenyl)-2-(3-(trifluoromethyl)phenylsulfonamido)propanoate (4m). The title compound was obtained from **4g** (0.05 g) as a white foam (0.036 g, 62%). R_f (ether/*n*-Hex 9:1) = 0.44. ^1H NMR (300 MHz, CDCl_3) δ 1.27 (s, 9 H), 1.5 (s, 9 H), 1.83 (m, 4 H), 2.13 (s, 3 H), 2.34 (s, 3 H), 2.87 (m, 1 H), 3.02 (m, 1 H), 4.02 (m, 5 H), 5.2 (d, $J = 9.4$ Hz, SO_2NH , 1 H), 6.68 (d, $J = 8.4$ Hz, 1 H), 6.79 (dd, $J = 8.4, 2$ Hz, 1 H), 6.85 (d, $J = 5$ Hz, 1 H), 7.39 (s, 1 H), 7.56 (t, $J = 7.9$ Hz, 1 H), 7.74 (d, $J = 7.9$ Hz, 1 H), 7.8 (br s, NHCO , 1 H), 7.94 (d, $J = 7.9$ Hz, 1 H), 8.02 (s, 1 H), 8.09 (d, $J = 2$ Hz, 1 H), 8.2 (d, $J = 5$ Hz, 1 H). ^{13}C NMR (75 MHz, CDCl_3) δ 21.34, 25.03, 25.86, 26.57, 27.9, 28.54, 38.96, 46.67, 57.42, 68.53, 81.2, 83.22, 110.82, 120.87, 121.04, 121.23, 124.4, 124.88, 127.66, 127.82, 129.1, 129.87, 130.81, 131.81, 141.45, 146.45, 147.47, 148.5, 154.5, 154.7, 167.19, 169.86, (CF_3 not visible). MS (ESI) m/z 787 $[\text{M} + \text{Na}]^+$, 765 $[\text{M} + \text{H}]^+$. HRMS $\text{C}_{37}\text{H}_{47}\text{F}_3\text{N}_4\text{O}_8\text{S}$ calcd for $[\text{M} + \text{Na}]^+$, 787.2964; found, 787.2935.

(S)-*t*-Butyl 3-(3-Acetamido-4-(3-(5,6,7,8-tetrahydro-1,8-naphthyridin-2-yl)propoxy)phenyl)-2-(3-(trifluoromethyl)phenylsulfonamido)propanoate (4n). The title compound was obtained from **4k** (0.1 g) as a white solid (0.07 g, 66%). R_f (acetone/*n*-Hex 8:2) = 0.56. IR 2955, 1731, 1651, 1327, 1159 cm^{-1} . ^1H NMR (300 MHz, CDCl_3) δ 1.26 (s, 9 H), 1.91 (m, 2 H), 2.17 (m + s, 5 H), 2.72 (m, 4 H), 2.86 (m, 1 H), 3.02 (m, 1 H), 3.39 (m, 2 H), 4.01 (t, $J = 6.4$ Hz, 2 H), 4.07 (m, 1 H), 4.85 (br s, SO_2NH , 1 H), 5.3 (br s, NH, 1 H), 6.36 (d, $J = 7.3$ Hz, 1 H), 6.7 (d, $J = 8.3$ Hz, 1 H), 6.79 (dd, $J = 8.3, 2$ Hz, 1 H), 7.08 (d, $J = 7.3$ Hz, 1 H), 7.54 (t, $J = 7.9$ Hz, 1 H), 7.73 (d, $J = 7.9$ Hz, 1 H), 7.85 (br s, CONH, 1 H), 7.93 (d, $J = 7.9$ Hz, 1 H), 8.02 (s, 1 H), 8.09 (d, $J = 2$ Hz, 1 H). ^{13}C NMR (75 MHz, CDCl_3) δ 19.44, 25.14, 26.55, 27.92, 29.22, 34.1, 39.01, 41.81, 57.41, 68.29, 83.24, 111.35, 111.52, 114.04, 120.99, 124.43, 124.85, 127.71, 128.05, 129.27, 129.89, 130.82, 131.9, 137.14, 141.46, 146.49, 155.94, 156.73, 168.37, 170.05 (CF_3 not visible). MS (ESI) m/z 675 $[\text{M} - \text{H}]^-$, 209. HRMS $\text{C}_{33}\text{H}_{39}\text{F}_3\text{N}_4\text{O}_6\text{S}$ calcd for $[\text{M} + \text{H}]^+$, 677.2621; found, 677.2606.

General Procedure for the Coupling of Spacer-Arms (Table 3). Acid **23** or **24** (see Scheme 1, 0.2 mmol) dissolved in DMF (1 mL) was treated successively with PyBOP (0.011 g, 0.2 mmol) and Et₃N (0.027 mL, 0.2 mmol) at 20 °C under Ar atmosphere. After 2 h, precursor **4** (0.18 mmol) dissolved in DMF (0.3 mL) was added dropwise with a syringe, and the mixture was stirred for 18 h at 20 °C. After dilution with brine (5 mL), the solution was extracted with ether (3 × 5 mL) and EtOAc (1 × 5 mL). The combined organic phases were washed with brine (5 mL), dried over MgSO₄, and concentrated under vacuum. The residue (brown oil) was purified by chromatography on silica gel.

(S)-*t*-Butyl 3-(3-(2-(2-(2-(2-(*t*-Butoxycarbonyl)aminoethoxy)ethoxy)ethoxy)acetamido)-4-(4-(4-methylpyridin-2-yl-*t*-butoxycarbonylamino)butoxy)phenyl)-2-(3-(trifluoromethyl)phenylsulfonamido)propanoate (6a). The title compound was obtained from **23a** (0.046 g) and **4g** (0.1 g) as a white foam (0.052 g, 37%). *R_f* (EtOAc/acetone 8:2) = 0.53. IR 2936, 1701, 1327, 1163 cm⁻¹. ¹H NMR (500 MHz, CDCl₃) δ 1.27 (s, 9 H), 1.44 (s, 9 H), 1.49 (s, 9 H), 1.84 (m, 4 H), 2.34 (s, 3 H), 2.88 (m, 1 H), 3.01 (m, 1 H), 3.28 (m, 2 H), 3.5 (t, *J* = 5.8 Hz, 2 H), 3.61–3.75 (m, 8 H), 4.02 (m, 4 H), 4.07 (m, 1 H), 4.12 (s, 2 H), 5.07 (br s, BocNH, 1 H), 5.32 (d, *J* = 10 Hz, SO₂NH, 1 H), 6.72 (d, *J* = 8.3 Hz, 1 H), 6.85 (dd, *J* = 8.3, 2 Hz, 1 H), 6.87 (d, *J* = 5.4 Hz, 1 H), 7.4 (s, 1 H), 7.57 (t, *J* = 7.8 Hz, 1 H), 7.75 (d, *J* = 7.8 Hz, 1 H), 7.95 (d, *J* = 7.8 Hz, 1 H), 8.02 (s, 1 H), 8.13 (d, *J* = 2 Hz, 1 H), 8.2 (d, *J* = 5.4 Hz, 1 H), 8.9 (br s, CONH, 1 H). ¹³C NMR (125 MHz, CDCl₃) δ 21.42, 25.53, 26.79, 27.91, 28.51, 28.64, 38.95, 40.52, 46.54, 57.39, 68.36, 70.37–71.2, 71.35, 81.43, 83.25, 111.12, 120.6, 120.98, 121.18, 124.41, 125.32, 127.13, 127.76, 129.31, 129.91, 130.81, 131.78, 141.47, 146.93, 147.12, 148.38, 154.38, 154.42, 156.22, 167.78, 169.94, (CF₃ not visible). MS (ESI) *m/z* 1010 [M – H]⁻, 910. HRMS C₄₈H₆₈F₃N₅O₁₃S calcd for [M + Na]⁺, 1034.4384; found, 1034.4384.

(S)-*t*-Butyl 3-(3-(2-(2-(2-(2-(2-(2-(*t*-Butoxycarbonyl) aminoethoxy)ethoxy)ethoxy)ethoxy)ethoxy)acetamido)-4-(4-(4-methylpyridin-2-yl-*t*-butoxycarbonylamino)butoxy)phenyl)-2-(3-(trifluoromethyl)phenylsulfonamido)propanoate (7a). The title compound was obtained from **23b** (0.171 g) and **4g** (0.219 g) as a pale yellow foam (0.165 g, 50%). *R_f* (EtOAc/acetone 9:1) = 0.57. IR 2932, 1700, 1541, 1327, 1163 cm⁻¹. ¹H NMR (500 MHz, CDCl₃) δ 1.25 (s, 9 H), 1.43 (s, 9 H), 1.49 (s, 9 H), 1.79 (m, 2 H), 1.85 (m, 2 H), 2.34 (s, 3 H), 2.88 (m, 1 H), 3.01 (m, 1 H), 3.3 (m, 2 H), 3.54 (t, *J* = 5.1 Hz, 2 H), 3.61–3.75 (m, 20 H), 4 (m, 4 H), 4.07 (m, 1 H), 4.17 (s, 2 H), 5.14 (br s, BocNH, 1 H), 5.44 (br s, SO₂NH, 1 H), 6.71 (d, *J* = 8.3 Hz, 1 H), 6.81 (dd, *J* = 8.3, 2 Hz, 1 H), 6.86 (d, *J* = 5.4 Hz, 1 H), 7.37 (s, 1 H), 7.58 (t, *J* = 7.8 Hz, 1 H), 7.75 (d, *J* = 7.8 Hz, 1 H), 7.92 (d, *J* = 7.8 Hz, 1 H), 8 (s, 1 H), 8.13 (s, 1 H), 8.2 (d, *J* = 5.4 Hz, 1 H), 8.7 (s, CONH, 1 H). ¹³C NMR (125 MHz, CDCl₃) δ 21.27, 25.56, 26.47, 27.82, 28.47, 28.53, 38.98, 40.29, 46.57, 57.48, 68.52, 69.7–70.78, 71.3, 79.53, 81.14, 83.21, 111.1, 120.94, 121.28, 122, 124.24, 125.39, 126.89, 127.55, 129.33, 130.02, 130.73, 131.76, 141.32, 147.03, 147.47, 148.51, 154.4, 154.7, 155, 167.19, 169.86, (CF₃ not visible). MS (ESI) *m/z* 1142 [M – H]⁻. HRMS C₅₄H₈₀F₃N₅O₁₆S calcd for [M + Na]⁺, 1166.5171; found, 1166.5159.

(S)-*t*-Butyl 3-(3-(2-(2-(2-(2-(*t*-Butoxycarbonyl)aminoethoxy)ethoxy)ethoxy)acetamido)-4-(3-(5,6,7,8-tetrahydro-1,8-naphthyridin-2-yl)propoxy)phenyl)-2-(3-(trifluoromethyl)phenylsulfonamido)propanoate (6b). The title compound was obtained from **23a** (0.058 g) and **4k** (0.110 g) as a white foam (0.059 g, 37%). *R_f* (EtOAc/acetone 6:4) = 0.57. IR 2931, 1684, 1327, 1161 cm⁻¹. ¹H NMR (500 MHz, CDCl₃) δ 1.26 (s, 9 H), 1.42 (s, 9 H), 1.91 (m, 2 H), 2.19 (m, 2 H), 2.71 (t, *J* = 6.2 Hz, 2 H), 2.75 (t, *J* = 7.4 Hz, 2 H), 2.85–3.04 (m, 2 H), 3.28 (m, 2 H), 3.41 (m, 2 H), 3.46–3.8 (m, 10 H), 3.98 (t, *J* = 6.4 Hz, 2 H), 4.01 (m, 1 H), 4.13 (s, 2 H), 5.05–5.4 (m, SO₂NH + BocNH, 2 H), 6.35 (d, *J* = 7.2 Hz, 1 H), 6.71 (d, *J* = 8.3 Hz, 1 H), 6.82 (d, *J* = 8.3 Hz, 1 H), 7.12 (d, *J* = 7.2 Hz, 1 H), 7.56 (t, *J* = 7.9 Hz, 1 H), 7.74 (d, *J* = 7.9 Hz, 1 H), 7.94 (d, *J* = 7.9 Hz, 1 H), 8.03 (s, 1 H), 8.14 (s, 1 H), 8.9 (br s, CONH + HN=C=N, 2 H). ¹³C NMR (75 MHz, CDCl₃) δ 21.23,

26.4, 27.88, 28.6, 29.12, 33.3, 38.83, 40.46, 41.76, 57.49, 67.83, 70.1–71, 83.23, 111.39, 111.56, 114.85, 121.71, 124.36, 125.53, 126.85, 127.8, 129.33, 129.98, 130.82, 131.72, 137.86, 141.46, 147.23, 155.27, 155.96, 156.61, 168.26, 169.65, (CF₃ not visible). MS (ESI) *m/z* 922 [M – H]⁻. HRMS C₄₄H₆₀F₃N₅O₁₁S calcd for [M + Na]⁺, 964.3860; found, 964.3831.

(S)-*t*-Butyl 3-(3-(2-(2-(2-(2-(2-(2-(*t*-Butoxycarbonyl) aminoethoxy)ethoxy)ethoxy)ethoxy)ethoxy)acetamido)-4-(3-(5,6,7,8-tetrahydro-1,8-naphthyridin-2-yl)propoxy)phenyl)-2-(3-(trifluoromethyl)phenylsulfonamido)propanoate (7b). The title compound was obtained from **23b** (0.171 g) and **4k** (0.344 g) as a very viscous colorless oil (0.187 g, 33%). *R_f* (EtOAc/acetone 1:1) = 0.6. IR 2926, 1704, 1327, 1161 cm⁻¹. ¹H NMR (500 MHz, CDCl₃) δ 1.26 (s, 9 H), 1.45 (s, 9 H), 1.89 (m, 2 H), 2.19 (m, 2 H), 2.69 (t, *J* = 6.2 Hz, 2 H), 2.74 (t, *J* = 7.4 Hz, 2 H), 2.86–3.02 (m, 2 H), 3.31 (m, 2 H), 3.39 (m, 2 H), 3.51–3.8 (m, 22 H), 3.99 (t, *J* = 6.4 Hz, 2 H), 4.07 (m, 1 H), 4.13 (s, 2 H), 4.85 (br s, BocNH, 1 H), 5.35 (br s, SO₂NH, 1 H), 6.36 (d, *J* = 7.3 Hz, 1 H), 6.7 (d, *J* = 8.3 Hz, 1 H), 6.79 (dd, *J* = 8.3, 2 Hz, 1 H), 7.08 (d, *J* = 7.3 Hz, 1 H), 7.54 (t, *J* = 7.9 Hz, 1 H), 7.73 (d, *J* = 7.9 Hz, 1 H), 7.85 (br s, CONH, 1 H), 7.93 (d, *J* = 7.9 Hz, 1 H), 8.02 (s, 1 H), 8.13 (d, *J* = 2 Hz, 1 H), 8.99 (br s, NH=C=N, 1 H). ¹³C NMR (75 MHz, CDCl₃) δ 21.61, 26.53, 27.86, 28.6, 29.22, 33.98, 38.88, 40.51, 41.74, 57.45, 67.91, 70.3–71.3, 83.12, 111.09, 111.55, 113.74, 120.74, 124.33, 125.18, 127.08, 127.67, 129.18, 129.83, 130.73, 131.72, 136.88, 141.49, 146.88, 156.06, 156.91, 156.93, 167.71, 170.03, (CF₃ not visible). MS (ESI) *m/z* 1054 [M – H]⁻. HRMS C₅₀H₇₂F₃N₅O₁₄S calcd for [M + H]⁺, 1056.4827; found, 1056.4845.

General Procedure for Boc Deprotection (Table 4). Boc-protected compound (0.1 g) dissolved in DCM (1 mL) was treated with TFA (1 mL) during 2 h at 20 °C. Concentration under vacuum quantitatively gave the peptidomimetic (for testing) as TFA salt. Compounds are stored in the fridge (–18 °C) as TFA salt. Neutralization could be performed by dissolution in DCM (0.1 g/5 mL DCM), washing with phosphate buffer (pH 8, 2 × 1 mL), drying (MgSO₄), and concentration (yellow oils).

(S)-3-(3-Amino-4-(4-(4-methylpyridin-2-ylamino)butoxy)phenyl)-2-(3-(trifluoromethyl)phenylsulfonamido)propanoic Acid (5g). ¹H NMR (500 MHz, CD₃OD) δ 1.96 (m, 4 H), 2.4 (s, 3 H), 2.86 (m, 1 H), 3.12 (m, 1 H), 3.44 (t, *J* = 6.6 Hz, 2 H), 4.11 (m, 1 H), 4.16 (t, *J* = 7.8 Hz, 2 H), 6.73 (dd, *J* = 6.7, 1.2 Hz, 1 H), 6.88 (s, 1 H), 7.04 (d, *J* = 8.4 Hz, 1 H), 7.22 (dd, *J* = 8.4, 2 Hz, 1 H), 7.25 (d, *J* = 2 Hz, 1 H), 7.69 (m, 2 H), 7.86 (d, *J* = 7.9 Hz, 1 H), 7.96 (d, *J* = 7.9 Hz, 1 H), 8.02 (s, 1 H). ¹³C NMR (125 MHz, CD₃OD) δ 22.81, 26.74, 28.24, 39.69, 43.71, 59.66, 70.35, 113.65, 114.66, 116.33, 121.28, 125.68, 126.78, 130.9, 131.93, 132.02, 132.4, 132.86, 133.35, 136.39, 144.49, 144.5, 153.12, 155.07, 174.34. HRMS C₂₆H₂₉F₃N₄O₅S calcd for [M + H]⁺, 567.1889; found, 567.1882.

(S)-3-(3-Amino-4-(5,6,7,8-tetrahydro-1,8-naphthyridin-2-yl)-butoxy)phenyl)-2-(3-(trifluoromethyl)phenylsulfonamido)propanoic Acid (5l). ¹H NMR (500 MHz, CD₃OD) δ 1.93 (m, 6 H), 2.83 (m, 5 H), 3.1 (m, 1 H), 3.49 (t, *J* = 5.6 Hz, 2 H), 4.1 (m, 1 H), 4.15 (m, 2 H), 6.63 (d, *J* = 7.3 Hz, 1 H), 7.05 (d, *J* = 9 Hz, 1 H), 7.25 (m, 2 H), 7.57 (d, *J* = 7.3 Hz, 1 H), 7.69 (t, *J* = 7.9 Hz, 1 H), 7.86 (d, *J* = 7.9 Hz, 1 H), 7.98 (d, *J* = 7.9 Hz, 1 H), 8.03 (s, 1 H). ¹³C NMR (125 MHz, CD₃OD) δ 21.38, 27.19, 27.34, 30.26, 34.1, 39.84, 43.06, 59.66, 70.36, 112.51, 114.62, 121.52, 124.64, 125.76, 126.59, 130.92, 132.04, 132.44, 132.96, 133.27, 143.63, 144.58, 150.58, 153.04, 153.76, 174.43, (C-CF₃ not visible). HRMS C₂₈H₃₁F₃N₄O₅S calcd for [M + H]⁺, 593.2046; found, 593.2022.

(S)-3-(3-Acetamido-4-(4-methylpyridin-2-ylamino)butoxy)phenyl)-2-(3-(trifluoromethyl)phenylsulfonamido)propanoic Acid (5m). ¹H NMR (500 MHz, CD₃OD) δ 1.93 (m, 4 H), 2.14 (s, 3 H), 2.38 (s, 3 H), 2.75 (m, 1 H), 3.02 (m, 1 H), 3.4 (t, *J* = 7 Hz, 2 H), 4.07 (m, 3 H), 6.73 (d, *J* = 6.6 Hz, 1 H), 6.8 (d, *J* = 8.5 Hz, 1 H), 6.82 (s, 1 H), 6.88 (dd, *J* = 8.5, 2.1 Hz, 1 H), 7.58 (m, 2 H), 7.67 (d, *J* = 6.6 Hz, 1 H), 7.8 (d, *J* = 7.9 Hz, 1 H), 7.85 (d, *J* = 7.9 Hz, 1 H), 7.95 (s, 1 H). ¹³C NMR (125 MHz, CD₃OD) δ 22.82, 24.55, 26.87, 28.31, 40, 43.72, 60, 69.83, 113.66, 113.67,

116.4, 125.54, 126.31, 128.38, 128.56, 130.58, 130.83, 131.9, 132.36, 133, 133.5, 136.26, 144.69, 151.07, 154.96, 172.63, 174.94, (CF₃ not visible). HRMS C₂₈H₃₁F₃N₄O₆S calcd for [M + H]⁺, 609.1995; found, 609.1998.

(S)-3-(3-Acetamido-4-(3-(5,6,7,8-tetrahydro-1,8-naphthyridin-2-yl)propoxy)phenyl)-2-(3-(trifluoromethyl)phenylsulfonamido)propanoic Acid (5n). ¹H NMR (500 MHz, CD₃OD) δ 1.92 (m, 2 H), 2.17 (s, 3 H), 2.21 (m, 2 H), 2.78 (m, 3 H), 2.91 (t, *J* = 7.4 Hz, 2 H), 3.02 (m, 1 H), 3.45 (t, *J* = 5.4 Hz, 2 H), 4.03 (t, *J* = 5.8 Hz, 2 H), 4.09 (m, 1 H), 6.63 (d, *J* = 7.4 Hz, 1 H), 6.77 (d, *J* = 8.4 Hz, 1 H), 6.9 (dd, *J* = 8.4, 1.8 Hz, 1 H), 7.56 (m, 2 H), 7.61 (t, *J* = 7.8 Hz, 1 H), 7.8 (d, *J* = 7.8 Hz, 1 H), 7.87 (d, *J* = 7.8 Hz, 1 H), 7.96 (s, 1 H). ¹³C NMR (125 MHz, CD₃OD) δ 21.3, 24.6, 27.25, 30.03, 31.2, 40.02, 43.14, 60, 68.57, 112.85, 113.58, 121.7, 125.63, 126.67, 128.43, 128.67, 130.64, 131.1, 131.9, 132.41, 133.05, 143.69, 144.71, 149.79, 151.08, 153.57, 172.8, 174.84, (CF₃ not visible). HRMS C₂₉H₃₁F₃N₄O₆S calcd for [M + H]⁺, 621.1995; found, 621.1985.

(S)-3-(3-(2-(2-(2-(2-Aminoethoxy)ethoxy)ethoxy)acetamido)-4-(4-(4-methylpyridin-2-ylamino)butoxy)phenyl)-2-(3-(trifluoromethyl)phenylsulfonamido)propanoic Acid (8a). ¹H NMR (500 MHz, CD₃OD) δ 1.93 (m, 2 H), 1.98 (m, 2 H), 2.38 (s, 3 H), 2.74 (m, 1 H), 3.05 (m, 3 H), 3.43 (t, *J* = 6.8 Hz, 2 H), 3.60–3.85 (m, 10 H), 4.08 (m, 3 H), 4.18 (s, 2 H), 6.73 (dd, *J* = 6.6, 1.3 Hz, 1 H), 6.84 (m, 2 H), 6.91 (dd, *J* = 8.3, 2 Hz, 1 H), 7.61 (t, *J* = 7.8 Hz, 1 H), 7.7 (d, *J* = 6.6 Hz, 1 H), 7.81 (d, *J* = 7.8 Hz, 1 H), 7.89 (d, *J* = 7.8 Hz, 1 H), 7.9 (bs, 2 H). ¹³C NMR (125 MHz, CD₃OD) δ 22.85, 26.84, 28.45, 40.13, 41.44, 43.66, 60.08, 68.79, 69.84, 71.8–72.9, 113.4, 113.41, 116.42, 123.65, 125.5, 127.97, 128.26, 130.61, 131.24, 131.89, 132.38, 133, 136.43, 144.6, 149.57, 155, 155.1, 171.3, 174.96, (CF₃ not visible). HRMS C₃₄H₄₅F₃N₅O₉S calcd for [M + H]⁺, 756.2890; found, 756.2886.

(S)-3-(3-(2-(2-(2-(2-Aminoethoxy)ethoxy)ethoxy)acetamido)-4-(3-(5,6,7,8-tetrahydro-1,8-naphthyridin-2-yl)propoxy)phenyl)-2-(3-(trifluoromethyl)phenylsulfonamido)propanoic Acid (8b). ¹H NMR (500 MHz, CD₃OD) δ 1.92 (m, 2 H), 2.14 (m, 2 H), 2.75 (t, *J* = 6.2 Hz, 2 H), 2.81 (m, 3 H), 2.96 (m, 1 H), 3.03 (t, *J* = 5.2 Hz, 2 H), 3.4 (t, *J* = 5.1 Hz, 2 H), 3.6–3.79 (m, 10 H), 3.88 (m, 1 H), 4.03 (t, *J* = 5.8 Hz, 2 H), 4.15 (s, 2 H), 6.59 (d, *J* = 7.3 Hz, 1 H), 6.78 (d, *J* = 8.3 Hz, 1 H), 6.9 (dd, *J* = 8.3, 2 Hz, 1 H), 7.44 (d, *J* = 7.4 Hz, 1 H), 7.62 (t, *J* = 7.8 Hz, 1 H), 7.8 (d, *J* = 7.8 Hz, 1 H), 7.89 (d, *J* = 2 Hz, 1 H), 7.96 (d, *J* = 7.8 Hz, 1 H), 8 (s, 1 H). ¹³C NMR (125 MHz, CD₃OD) δ 21.46, 27.36, 30.36, 31.49, 40.79, 41.38, 42.75, 61.6, 68.8, 69.19, 72.09–72.84, 112.23, 113.28, 120.93, 124.05, 125.62, 128.1, 128.17, 130.63, 131.7, 131.99, 132.59, 142.79, 144.47, 149.23, 150.61, 155.06, 171.14, 177.99, (C-CF₃ not visible). HRMS C₃₅H₄₄F₃N₅O₁₉S calcd for [M + H]⁺, 768.2890; found, 768.2883.

(S)-3-(3-(20-Amino-3,6,9,12,15,18-hexaoxaicosanamide)-4-(4-(4-methylpyridin-2-ylamino)butoxy)phenyl)-2-(3-(trifluoromethyl)phenylsulfonamido)propanoic Acid (9a). ¹H NMR (500 MHz, CD₃OD) δ 1.93–1.99 (m, 4 H), 2.38 (s, 3 H), 2.74 (m, 1 H), 3.05 (m, 3 H), 3.13 (t, *J* = 5 Hz, 2 H), 3.43 (m, 2 H), 3.59–3.81 (m, 20 H), 4.08 (m, 3 H), 4.18 (s, 2 H), 6.73 (dd, *J* = 6.5, 1.3 Hz, 1 H), 6.83 (m, 2 H), 6.91 (m, 1 H), 7.61 (m, 1 H), 7.7 (m, 1 H), 7.8 (d, *J* = 7.8 Hz, 1 H), 7.86 (d, *J* = 7.8 Hz, 1 H), 7.9 (m, 2 H). ¹³C NMR (125 MHz, CD₃OD) δ 22.85, 26.87, 28.45, 40.13, 41.52, 43.68, 60.11, 68.76, 69.84, 71.8–72.88, 113.4, 113.42, 116.42, 123.57, 125.5, 127.93, 128.26, 130.61, 131.18, 131.9, 132.37, 132.95, 136.43, 144.7, 149.54, 154.9, 154.94, 171.28, 174.94, (CF₃ not visible). HRMS C₄₀H₅₆F₃N₅O₁₂S calcd for [M + H]⁺, 888.3677; found, 888.3674.

(S)-3-(3-(20-Amino-3,6,9,12,15,18-hexaoxaicosanamide)-4-(3-(5,6,7,8-tetrahydro-1,8-naphthyridin-2-yl)propoxy)phenyl)-2-(3-(trifluoromethyl)phenylsulfonamido)propanoic Acid (9b). ¹H NMR (300 MHz, CD₃OD) δ 1.87 (m, 2 H), 2.15 (m, 2 H), 2.73 (m, 5 H), 3.01 (m, 1 H), 3.11 (t, *J* = 5.1 Hz, 2 H), 3.38 (t, *J* = 5.3 Hz, 2 H), 3.54–3.87 (m, 22 H), 4.03 (m, 3 H), 4.18 (s, 2 H), 6.45 (d, *J* = 7.2 Hz, 1 H), 6.76 (d, *J* = 8.4 Hz, 1 H), 7.26 (d, *J* = 8.4 Hz, 1 H), 7.27 (d, *J* = 7.2 Hz, 1 H), 7.6 (t, *J* = 7.5 Hz, 1 H),

7.77 (d, *J* = 7.5 Hz, 1 H), 7.93 (m, 3 H). ¹³C NMR (75 MHz, CD₃OD) δ 22.32, 27.81, 30.79, 33.35, 41.06, 41.51, 42.99, 61.99, 68.78, 69.48, 72.76–72.81, 112.57, 113.28, 118.78, 123.47, 125.63, 128.02, 128.06, 130.6, 131.64, 131.99, 132.24, 132.92, 141.11, 144.54, 149.23, 154.25, 156.16, 171.14, 177.99, (CF₃ not visible). HRMS C₄₁H₅₆F₃N₅O₁₂S calcd for [M + H]⁺, 900.3677; found, 900.3699.

Evaluations. Binding to Isolated Integrins. The human α_vβ₃ integrins (purified from placenta) were purchased from Chemicon International Inc. (Temecula, CA), and α_{IIB}β₃ integrins were purified from platelets by affinity chromatography, as described.⁸² The integrins were diluted to 500 ng/mL (α_vβ₃) or 1 μg/mL (α_{IIB}β₃) in a Tris binding buffer (2 mM CaCl₂, 1 mM MgCl₂ and MnCl₂, pH 7.5), and adsorbed onto 96-well Costar (Bethesda, MD) binding plates (100 μL per well). After a one-hour incubation at room temperature, the plates were incubated for another hour with a blocking solution of 1% albumin to prevent nonspecific binding. The plates were then washed three times in binding buffer containing 0.1% albumin. The physiological ligands vitronectin (BD Biosciences, Le Pont de Claix, France) for α_vβ₃ and fibrinogen (Sigma) for α_{IIB}β₃ were labeled with *N*-hydroxysuccinimido-biotin. Stock solutions of compounds were solubilized at 10 mM in dimethylsulfoxide (DMSO). All compounds were aliquoted and stored at -20 °C. Adsorbed integrins were then incubated for 30 min with their corresponding soluble biotinylated ligand in excess, in the binding buffer containing 0.1% albumin and in the presence of various concentrations of tested compounds. After several washings, the amount of bound ligands was indirectly estimated after the sequential incubation with an antibody against biotin coupled to alkaline phosphatase and *para*-nitrophenyl phosphate for readout at 405 nm in a colorimetric assay. The concentration of compound corresponding to 50% inhibition (IC₅₀) was inferred from the dose–response curves of at least two pooled experiments and used to compare the products.

Human Osteoprogenitor (HOP) Cell Cultures. HOP cells were isolated from human bone marrow stromal cells (HBMSC) according to Vilamitjana et al.,⁸³ with some modifications.⁸⁴ Briefly, human bone marrow was obtained by aspiration from the iliac crest of healthy donors (30–70 y/o) undergoing hip prosthesis surgery after traumatic shock. Cells were separated into single suspension by sequentially passing the suspension through syringes fitted with 16, 18, and 21 gauge needles. After centrifugation for 15 min at 800g, the pellet was resuspended in Iscove Modified Dulbecco's Medium (IMDM, Gibco) supplemented with 10% (v/v) fetal calf serum (FCS, Gibco) and 10⁻⁸ M dexamethasone (Sigma). Cells were then plated into 75 cm² cell culture flasks (Nunc) and incubated in a humidified atmosphere of 95% air and 5% CO₂ at 37 °C. For two weeks, the complete medium was supplemented with 10⁻⁸ dexamethasone and then every 3 days with IMDM containing 10% FCS (v/v). Subculturing was performed using 0.2% (w/v) trypsin, 5 mM EDTA. Cells arising from the second subculture were used in these experiments to get a homogeneous cell population in terms of cell phenotype. Alkaline phosphatase and *Chfal/runx2* gene expression were assessed by real time quantitative PCR to control the osteoblastic phenotype.

Competition and Cell Adhesion Assay. The 96-well polystyrene plates (Nunc) were coated with vitronectin from human plasma (Sigma) dissolved at 5 μg/mL in IMDM 1 mM CaCl₂. The coated plates (30 μL per well) were conditioned 2 h at 37 °C and then rinsed in PBS before use. Peptidomimetics were prepared at the following final concentrations: 10⁻⁴, 10⁻⁶, 10⁻⁸, 10⁻¹⁰, 10⁻¹² M. HOP (32000 cells/mL) were incubated with peptidomimetics 5g, 5n, and 8b in serum-free IMDM to saturate the integrin receptors on the cell surface for 1 h at 37 °C under gentle shaking before seeding. For each competition assay, 100 μL of the cell suspension were inoculated onto the vitronectin-coated well, and the competitive adhesion was allowed to take place for 30 min at 37 °C.

Cell attachment was measured by a modified colorimetric method according to Landegren et al.⁷⁰ After the nonadherent cells were removed by washings with PBS 0.1 M pH 7.4, 500 μ L of chromogenic substrate solution (7.5 mM substrate (*p*-nitrophenyl *N*-acetyl β -D-glucosaminide); 0.1 M Na citrate; pH = 5; 5% (v/v) Triton-X 100) were added for 2 h at 37 °C in humidified atmosphere. The reaction was stopped with 5 mM EDTA/ 50 mM glycine pH 10.4. The resulting chromophore was measured spectrophotometrically at 405 nm. The controls of cell adhesion were the followings: cells nonincubated in the presence of peptidomimetics then inoculated on culture plates coated with vitronectin (positive controls) and cells incubated in the presence of GRGDS (Sigma) at the same final concentrations then seeded on coated plates. Experiments were performed at least twice ($n = 6$ wells per concentration). Results are expressed as absorbance ratios of positive controls.

The U Mann–Whitney nonparametric test was used to test significance ($p < 0.05$).

Calculations. The geometry of the molecules has been fully optimized at the RHF level using the polarized double ζ basis set 6-31G(d)⁸⁵ and the minimal basis MINI-1' for the compound **8a** and **8b**.⁸⁶ All the calculations have been performed with the Gaussian 03 program.⁸⁷

Cell Culture System. Substrate Functionalization. Track-etched microporous membrane of PET (cyclopore) used as cell culture support was purchased from Whatman SA (Louvain-la-Neuve, Belgium). Samples for surface modification were cut in disks of 13 mm diameter and placed in a 24-well PS plate. Samples were washed with acetonitrile (ACN) (1 mL/sample, 10 min shaking) then activated by immersion in a freshly prepared 1 M solution of trifluorotriazine (1 mL/sample) for 2 or 3 h at 30 or 40 °C. After washing with ACN, the samples were incubated in a 10⁻³ M solution of adhesive molecules (graftable peptidomimetics and pentapeptide GRGDS) in phosphate buffer pH 8 (PB)-ACN (1:1, v/v; 1 mL/sample) for 17 h at 20 °C. The samples were washed successively (1 mL/sample) with PB-ACN, H₂O-ACN, 1 N HCl-ACN, and H₂O-ACN. For XPS analysis, samples were dried under high vacuum. Blank samples were prepared as above, but with omitting either the activation step, or the incubation step. The analyses were performed on a Kratos Axis Ultra spectrometer (Kratos Analytical, Manchester, UK) as previously described.⁸⁸ The derivatization rates were calculated from the experimental F/C atomic ratios (for peptidomimetics) and the N/C atomic ratio (for pentapeptide).⁴³ Results of covalent grafting were validated by comparison with the blank samples showing less than 0.01% of contamination by adsorbed peptidomimetic/peptide.

Endothelial Cell Culture. Mature endothelial cells were isolated from human saphenous veins (HSVEC) collected after surgical coronary bypass according to the French legislation. The samples were kept in Hanks' balanced salt solution supplemented with heparin (50 UI/mL; Sanofi Synthelabo, Paris, France) and transferred to the laboratory for isolation of endothelial cells. Cells were harvested as described by Golledge et al.⁸⁹ The isolated cells were seeded on culture flasks coated with 0.2% gelatin (w/v) and grown in a complete culture medium composed of M199 medium with glutamax (Invitrogen Corp, Gergy Pontoise, France) supplemented with 20% FCS (Eurobio, les Ulis, France), heparin 50 IU/mL (Sanofi Synthelabo, Paris, France), gentamycin 50 μ g/mL (Biomedica, Bousens, France), 10 ng/mL bFGF (Sigma Aldrich, St Quentin Fallavier, France). Media were changed three times a week. Cells were used for attachment experiments at passage 4.

Endothelial Cell Attachment. A pool of HSV cells from three donors was used. Disks of native and functionalized PET membranes were sterilized with ethanol (70%, 10 min), rinsed with phosphate buffered saline (PBS) three times (0.1 M, pH 7.4), and placed in 24-well tissue culture plates (Corning); samples were immobilized by the mean of glass rings. HSVECs were seeded on the surface of PET disks at the density of 5 \times 10⁴

cells/cm² in serum-free medium DMEM (Dulbecco's Modified Eagle Medium without phenol red), for 1, 3, and 6 h ($n = 3$). For each incubation time, cell attachment was measured by a colorimetric method according to Landegren et al.⁷⁰ with some modifications. The nonadherent cells were removed by washing with PBS 0.1 M pH 7.4. Chromogenic substrate solution of 500 μ L (see above, HOP assay) was added for 2 h at 37 °C in humidified atmosphere. Reaction was stopped (see above, HOP assay), and the resulting chromophore was measured spectrophotometrically at 405 nm. The positive and negative controls for cell adhesion were the native tissue culture PET and the tissue culture polystyrene (TCPS) coated with agarose (2%) respectively. Results of Figure 8 are expressed as % of absorbance considering native PET as 100%. The U Mann–Whitney nonparametric test was used to test significance.

Acknowledgment. This work was supported by the FRS-FNRS (Belgium) and FRIA-FNRS (Belgium), and by UCL (Louvain-la-Neuve) and ULg (Sart-Tilman) for computational facilities. V.R. is FRIA fellow, and G.D. and J.M.-B. are senior research associates of FRS-FNRS. Sabrina Devouge (UCL) and Annie Genton (Servier) are acknowledged for technical assistance.

Supporting Information Available: Large scale synthesis of precursor **1** (*t*-butyl 3-(4-hydroxy-3-nitro-phenyl)-2 (*S*)-(3-trifluoromethyl-benzene sulfonylamino)propionate) and HPLC control of its enantiomeric purity, synthesis of ω -functionalized propanols and butanols bearing the basic groups (or precursors of Arg-mimics) and their spectroscopic data (**10a**, **10b**, **12a**, **12b**, **13a**, **13b**, **14a**, **14b**, **15a**, **15b**, **16a**, **16b**, **17a**, **17b**, **18a**, **18b**, **19a**, **19b**, **21**, **22**; see Scheme 2), the synthesis and characterization of the OEG spacer-arms (**23a**, **23b**, **24**) and the complete descriptions of compounds cited in Tables 1–4 (except those included in the Experimental Section—Chemistry) are provided. Details of computational studies on cilengitide are also given). This material is available free of charge via the Internet at <http://pubs.acs.org>.

References

- Pierschbacher, M. D.; Ruoslahti, E. Cell attachment activity of fibronectin can be duplicated by small synthetic fragments of the molecule. *Nature* **1984**, *309*, 30–33.
- Ruoslahti, E. The RGD story: a personal account. *Matrix Biol.* **2003**, *22*, 459–465.
- Tamkun, J. W.; DeSimone, D. W.; Fonda, D.; Patel, R. S.; Buck, C.; Horwitz, A. F.; Hynes, R. O. Structure of integrin, a glycoprotein involved in the transmembrane linkage between fibronectin and actin. *Cell* **1986**, *46*, 271–282.
- Humphries, M. J. Integrin structure. *Biochem. Soc. Trans.* **2000**, *28*, 311–340.
- Takagi, J.; Petre, B. M.; Walz, T.; Springer, T. A. Global conformational rearrangements in integrin extracellular domains in outside-in and outside-out signaling. *Cell* **2002**, *110*, 599–611.
- Hynes, R. O. Integrins: bidirectional, allosteric signaling machines. *Cell* **2002**, *110*, 673–687.
- Brooks, P. C.; Clark, R. A. F.; Cheresh, D. A. Requirement of vascular integrin $\alpha_v\beta_3$ for angiogenesis. *Science* **1994**, *264*, 569–571.
- Duong, L. T.; Rodan, G. A. Integrin-mediated signaling in the regulation of osteoclast adhesion and activation. *Front. Biosci.* **1998**, *3*, d757–d768.
- Petitclerc, E.; Stromblad, S.; Von Schakscha, T. L.; Mitjans, F.; Piutlats, J.; Montgommery, A. M.; Cheresh, D. A.; Brooks, P. C. Integrin $\alpha_v\beta_3$ promotes M21 melanoma growth in human skin by regulating tumor cell survival. *Cancer Res.* **1999**, *59*, 2724–2730.
- Kumar, C. C. Integrin $\alpha_v\beta_3$ as a therapeutic target for blocking tumor-induced angiogenesis. *Curr. Drug Targets* **2003**, *4*, 123–131.
- Dechantstreiter, M. A.; Planker, E.; Mathae, B.; Lohof, E.; Hoelzemann, G.; Jonczyk, A.; Goodman, S. L.; Kessler, H. *N*-Methylated cyclic RGD peptides as highly active and selective $\alpha_v\beta_3$ integrin antagonists. *J. Med. Chem.* **1999**, *42*, 3033–3040.
- Keenan, R. M.; Miller, W. H.; Kwon, C.; Ali, F. E.; Callahan, J. F.; Calvo, R. R.; Hwang, S.-M.; Kopple, K. D.; Peishoff, C. E.;

- Samanen, J. M.; Wong, A. S.; Yuan, C.-K.; Huffman, W. F. Discovery of potent nonpeptide vitronectin receptor ($\alpha_v\beta_3$) antagonists. *J. Med. Chem.* **1997**, *40*, 2289–2292.
- (13) Miller, W. H.; Keenan, R. M.; Willette, R. N.; Lark, M. W. Identification and in vivo efficacy of small-molecule antagonists of integrin $\alpha_v\beta_3$ (the vitronectin receptor). *Drug Discovery Today* **2000**, *5*, 397–408.
- (14) Kerr, J. S.; Slee, A. M.; Mousa, S. A. The α_v integrin antagonists as novel anticancer agents: an update. *Expert Opin. Investig. Drugs* **2002**, *11*, 1765–1774.
- (15) Coleman, P. J.; Brashear, K. M.; Askew, B. C.; Hutchinson, J. H.; McVean, C. A.; Duong, L. T.; Feuston, B. P.; Fernandez-Metzler, C.; Gentile, M. A.; Hartman, G. D.; Kimmel, D. B.; Leu, C.-T.; Lipfert, L.; Merkle, K.; Pennypacker, B.; Prueksaritanont, T.; Rodan, G. A.; Wesolowski, G. A.; Rodan, S. B.; Duggan, M. E. Nonpeptide $\alpha_v\beta_3$ antagonists. Part 11: Discovery and preclinical evaluation of potent $\alpha_v\beta_3$ antagonists for the prevention and treatment of osteoporosis. *J. Med. Chem.* **2004**, *47*, 4829–4837.
- (16) Dayam, R.; Aiello, F.; Deng, J.; Wu, Y.; Garofalo, A.; Chen, X.; Neamati, N. Discovery of small molecule integrin $\alpha_v\beta_3$ antagonists as novel anticancer agents. *J. Med. Chem.* **2006**, *49*, 4526–4534.
- (17) Thumshirn, G.; Hersel, U.; Goodman, S. L.; Kessler, H. Multimeric cyclic RGD peptides as potential tools for tumor targeting: solid-phase peptide synthesis and chemoselective oxime ligation. *Chem.—Eur. J.* **2003**, *9*, 2717–2725.
- (18) Nasongkla, N.; Shuai, X.; Ai, H.; Weinberg, B. D.; Pink, J.; Boothman, D. A.; Gao, J. cRGD-functionalized polymer micelles for targeted doxorubicin delivery. *Angew. Chem., Int. Ed.* **2004**, *43*, 6323–6327.
- (19) Temming, K.; Schiffelers, R. M.; Molema, G.; Kok, R. J. RGD-based strategies for selective delivery of therapeutics and imaging agents to the tumour vasculature. *Drug Resist. Updates* **2005**, *8*, 381–402.
- (20) Hersel, U.; Dahmen, C.; Kessler, H. RGD modified polymers: biomaterials for stimulated cell adhesion and beyond. *Biomaterials* **2003**, *24*, 4385–4415.
- (21) Siebers, M. C.; ter Brugge, P. J.; Walboomers, X. F.; Jansen, J. A. Integrins as linker proteins between osteoblasts and bone replacing materials. A critical review. *Biomaterials* **2005**, *26*, 137–146.
- (22) Lieb, E.; Hacker, M.; Tessmar, J.; Kunz-Schughart, L. A.; Fiedler, J.; Dahmen, C.; Hersel, U.; Kessler, H.; Schulz, M. B.; Göpferich, A. Mediating specific cell adhesion to low-adhesive diblock copolymers by instant modification with cyclic RGD peptides. *Biomaterials* **2005**, *26*, 2333–2341.
- (23) Ma, P. X. Biomimetic materials for tissue engineering. *Adv. Drug Delivery Rev.* **2008**, *60*, 184–198.
- (24) Marchand-Brynaert, J.; Detrait, E.; Noiset, O.; Boxus, T.; Schneider, Y.-J.; Remacle, C. Biological evaluation of RGD peptidomimetics, designed for the covalent derivatization of cell culture substrata, as potential promoters of cellular adhesion. *Biomaterials* **1999**, *20*, 1773–1782.
- (25) Biltresse, S.; Attolini, M.; Marchand-Brynaert, J. Cell adhesive PET membranes by surface grafting of RGD peptidomimetics. *Biomaterials* **2005**, *26*, 4576–4587.
- (26) Li, L.-S.; Rader, C.; Matsushita, M.; Das, S.; Barbas, C. F.; Lerner, R. A.; Sinha, S. C. Chemical adaptor immunotherapy: design, synthesis, and evaluation of novel integrin-targeting devices. *J. Med. Chem.* **2004**, *47*, 5630–5640.
- (27) Meyer, A.; Auernheimer, J.; Modlinger, A.; Kessler, H. Targeting RGD recognizing integrins: drug development, biomaterial research, tumor imaging and targeting. *Curr. Pharm. Des.* **2006**, *12*, 2723–2747.
- (28) Patel, S.; Thakar, R. G.; Wong, J.; McLeod, S. D.; Li, S. Control of cell adhesion on poly(methyl methacrylate). *Biomaterials* **2006**, *27*, 2890–2897.
- (29) Auernheimer, J.; Zukowski, D.; Dahmen, C.; Kantlehner, M.; Enderle, A.; Goodman, S. L.; Kessler, H. Titanium implant materials with improved biocompatibility through coating with phosphate-anchored cyclic RGD peptides. *ChemBioChem* **2005**, *6*, 2034–2040.
- (30) Dahmen, C.; Auernheimer, J.; Meyer, A.; Enderle, A.; Goodman, S. L.; Kessler, H. Improving implant materials by coating with nonpeptidic, highly specific integrin ligands. *Angew. Chem., Int. Ed.* **2004**, *43*, 6649–6652.
- (31) Curley, G. P.; Blum, H.; Humphries, M. J. Integrin antagonists. *Cell. Mol. Life, Sci.* **1999**, *56*, 427–441.
- (32) Hartman, G. D.; Egbertson, M. S.; Halzenko, W.; Laswell, W. L.; Duggan, M. E.; Smith, R. L.; Naylor, A. M.; Manno, P. D.; Lynch, R. J.; Zhang, G.; Chang, C. T.-C.; Gould, R. J. Non-peptide fibrinogen receptor antagonists. I. Discovery and design of exosite inhibitors. *J. Med. Chem.* **1992**, *35*, 4640–4642.
- (33) Boxus, T.; Touillaux, R.; Dive, G.; Marchand-Brynaert, J. Synthesis and evaluation of RGD peptidomimetics aimed at surface bioderivatization of polymer substrates. *Bioorg. Med. Chem.* **1998**, *6*, 1577–1595.
- (34) Biltresse, S.; Attolini, M.; Dive, G.; Cordi, A.; Tucker, G. C.; Marchand-Brynaert, J. Novel RDG-like molecules based on the tyrosine template: design, synthesis, and biological evaluation on isolated integrins $\alpha_v\beta_3/\alpha_{IIb}\beta_3$ and in cellular adhesion tests. *Bioorg. Med. Chem.* **2004**, *12*, 5379–5393.
- (35) Yamanaka, T.; Ohkudo, M.; Kuroda, S.; Nakamura, H.; Takahashi, F.; Aoki, T.; Mihara, K.; Seki, J.; Kato, M. Design, synthesis, and structure–activity relationships of potent GPIIb/IIIa antagonists: discovery of FK419. *Bioorg. Med. Chem.* **2005**, *13*, 4343–4352.
- (36) Duggan, M. E.; Duong, L. T.; Fisher, J. E.; Hamill, T. G.; Hoffman, Huff, W. F. J. R.; Ihle, N. C.; Leu, C.-T.; Nagy, R. M.; Perkins, J. J.; Rodan, S. B.; Wesolowski, G.; Whitman, D. B.; Zartman, A. E.; Rodan, G. A.; Hartman, G. D. Nonpeptide $\alpha_v\beta_3$ Antagonists. 1. Transformation of a Potent, Integrin-Selective $\alpha_{IIb}\beta_3$ Antagonist into a Potent $\alpha_v\beta_3$ Antagonist. *J. Med. Chem.* **2000**, *43*, 3736–3745.
- (37) Rockwell, A. L.; Rafalski, M.; Pitts, W. J.; Batt, D. G.; Petraitis, J. J.; DeGrado, W. F.; Mousa, S.; Jadhav, P. K. Rapid synthesis of RGD mimetics with isoxazoline scaffolds on solid phase: identification of $\alpha_v\beta_3$ antagonists lead compounds. *Bioorg. Med. Chem. Lett.* **1999**, *9*, 937–942.
- (38) Duggan, M. E.; Hutchinson, J. H. Ligands to the integrin receptor $\alpha_v\beta_3$. *Expert Opin. Ther. Pat.* **2000**, *10*, 1367–1383.
- (39) Coleman, P. J.; Duong, L. T. Ligands to the integrin receptor $\alpha_v\beta_3$. *Expert Opin. Ther. Pat.* **2002**, *12*, 1009–1021.
- (40) Cacciari, B.; Spalluto, G. Non peptidic $\alpha_v\beta_3$ antagonists: Recent developments. *Curr. Med. Chem.* **2005**, *12*, 51–70.
- (41) Pilkington-Miksa, M. A.; Sarkar, S.; Writer, M. J.; Barker, S. E.; Shamlou, P. A.; Hart, S. L.; Hailes, H. C.; Tabor, A. B. Synthesis of bifunctional integrin-binding peptides containing PEG spacers of defined length for nonviral gene delivery. *Eur. J. Org. Chem.* **2008**, 2900–2914.
- (42) Heckmann, D.; Meyer, A.; Laufer, B.; Zahn, G.; Stragies, R.; Kessler, H. Rational design of highly active and selective ligands for the $\alpha_5\beta_1$ integrin receptor. *ChemBioChem* **2008**, *9*, 1397–1407.
- (43) Biltresse, S.; Descamps, D.; Henneuse-Boxus, C.; Marchand-Brynaert, J. Effect of the chemical nature and the length of spacer-arms on the covalent grafting of molecular probes at the surface of PET membranes. *J. Polym. Sci., Part A: Polym. Chem.* **2002**, *40*, 770–781.
- (44) Penso, M.; Albanese, D.; Landini, D.; Lupi, V.; Tricarico, G. Specific solvation as a tool for the N-chemoselective arylsulfonylation of tyrosine and (4-hydroxyphenyl)glycine methyl esters. *Eur. J. Org. Chem.* **2003**, 4513–4517.
- (45) Brennauer, A.; Keller, M.; Freund, M.; Bernhardt, G.; Buschauer, A. Decomposition of 1-(ω -aminoalkanoyl)guanidines under alkaline conditions. *Tetrahedron Lett.* **2007**, *48*, 6996–6999.
- (46) Nguyen, C.; Ruda, G. F.; Schipani, A.; Kasinathan, G.; Leal, I.; Musso-Buendia, A.; Kaiser, H.; Brun, R.; Ruiz-Perez, L. M.; Sahlberg, B.-L.; Johanson, N. G.; Gonzalez-Pacanoska, D.; Gilbert, I. Acyclic Nucleoside Analogues as Inhibitors of *Plasmodium falciparum* dUTPase. *J. Med. Chem.* **2006**, *49*, 4183–4195.
- (47) Kim, K. S.; Qian, L. Fire-retardant and intumescent compositions for cellulosic material. *Tetrahedron Lett.* **1993**, *34*, 7677–7680.
- (48) Frederick, R.; Charlier, C.; Robert, S.; Wouters, J.; Masereel, B.; Pochet, L. Investigation of mechanism-based thrombin inhibitors: Implications of a highly conserved water molecule for the binding of coumarins within the S pocket. *Bioorg. Med. Chem. Lett.* **2006**, *16*, 2017–2021.
- (49) Botta, M.; Corelli, F.; Maga, G.; Manetti, F.; Renzulli, M.; Spadari, S. Research on anti-HIV-1 agents. Part 2: Solid-phase synthesis, biological evaluation and molecular modeling studies of 2,5,6-trisubstituted-4(3H)-pyrimidines targeting HIV-1 reverse transcriptase. *Tetrahedron* **2001**, *57*, 8357–8367.
- (50) Marugan, J. J.; Manthey, C.; Analerio, B.; Lafrance, L.; Lu, T.; Markotan, T.; Leonard, K. A.; Crysler, C.; Eisennagel, S.; Dasgupta, M.; Tomczuk, B. Design, Synthesis, and Biological Evaluation of Novel Potent and Selective $\alpha_v\beta_3/\alpha_{IIb}\beta_3$ Integrin Dual Inhibitors with Improved Bioavailability. Selection of the Molecular Core. *J. Med. Chem.* **2005**, *48*, 926–934.
- (51) Geneste, H.; Kling, A.; Lauterbach, A.; Graef, C. I.; Subkowski, T.; Hornberger, W. Preparation of dibenzo[b,e]azepines as $\alpha_v\beta_3$ integrin ligands. Int. Patent WO 2002014320, **2002**.
- (52) Heckmann, D.; Meyer, A.; Marinelli, L.; Zahn, G.; Stragies, R.; Kessler, H. Probing integrin selectivity: rational design of highly active and selective ligands for the $\alpha_5\beta_1$ and $\alpha_v\beta_3$ integrin receptor. *Ang. Chem., Int. Ed.* **2007**, *46*, 3571–3574.
- (53) Lefrançois, J. M.; Heckmann, B. Preparation of pyrimidine amino acid derivatives as antagonists of the vitronectin receptor. French Patent FR 2870541, **2005**.

- (54) Dormer, P. G.; Eng, K. K.; Farr, R. N.; Humphrey, G. R.; McWilliams, J. C.; Reider, P. J.; Sager, J. W.; Volante, R. P. Highly Regioselective Friedlaender Annulations with Unmodified Ketones Employing Novel Amine Catalysts: Syntheses of 2-Substituted Quinolines, 1,8-Naphthyridines, and Related Heterocycles. *J. Org. Chem.* **2003**, *68*, 467–477.
- (55) Ameer, F.; Giles, R. G. F.; Green, I. R.; Nagabhushana, K. S. The DDQ mediated cyclization products of some 2-hydroxy-3-(1'-alkenyl)-1,4-naphthoquinones. *Synth. Commun.* **2002**, *32*, 369–380.
- (56) Backes, J. R.; Koert, U. Stereoselective synthesis of the monomeric unit of SCH 351448. *Eur. J. Org. Chem.* **2006**, 2777–2785.
- (57) Prabhakaran, P. C.; Gould, S. J.; Orr, G. R.; Coward, J. K. Synthesis of chirally deuteriated phthalimido-propanols and evaluation of their absolute stereochemistry. *J. Am. Chem. Soc.* **1988**, *110*, 5779–5784.
- (58) Kim, K. S.; Song, Y. H.; Lee, B. H.; Hahn, C. S. Efficient and selective cleavage of acetals and ketals using ferric chloride adsorbed on silica gel. *J. Org. Chem.* **1986**, *51*, 404–406.
- (59) Yong, Y. F.; Kowalski, J. A.; Lipton, M. A. Facile and Efficient Guanlylation of Amines Using Thioureas and Mukaiyama's Reagent. *J. Org. Chem.* **1997**, *62*, 1540–1542.
- (60) Balicki, R.; Maciejewski, G. A mild and selective deoxygenation of *N*-oxides with ammonium formate as a catalytic hydrogen transfer agent. *Synth. Commun.* **2002**, *32*, 1681–1683.
- (61) Salvagnini, C.; Gharbi, S.; Boxus, T.; Marchand-Brynaert, J. Synthesis and evaluation of a small library of graftable thrombin inhibitors derived from (L)-arginine. *Eur. J. Med. Chem.* **2007**, *42*, 37–53.
- (62) Momtaz, M.; Rerat, V.; Gharbi, S.; Gerard, E.; Pourcelle, V.; Marchand-Brynaert, J. A graftable LDV peptidomimetic: design, synthesis and application to a blood filtration membrane. *Bioorg. Med. Chem. Lett.* **2008**, *18*, 1084–1090.
- (63) Takahashi, T.; Shiyama, T.; Hosoya, K.; Tanaka, A. Development of chemically stable solid phases for the target isolation with reduced nonspecific binding proteins. *Bioorg. Med. Chem. Lett.* **2006**, *16*, 447–450.
- (64) Adamczyk, M.; Fishpaugh, J. R.; Thiruvazhi, M. Concise synthesis of *N*-protected carboxyalkyl ether amines. *Org. Prep. Proc. Int.* **2002**, *34*, 326–331.
- (65) Chapman, R. G.; Ostuni, E.; Liang, M. N.; Yan, L.; Whitesides, G. M. Self-assembled monolayer surfaces that resist the adsorption of biological species. Int. Patent WO 2002006407, **2002**.
- (66) Martinez, V.; Mecking, S.; Tassaing, T.; Besnard, M.; Moisan, S.; Moisan, S.; Cansell, F.; Aymonier, C. Dendritic core-shell macromolecules soluble in supercritical carbon dioxide. *Macromolecules* **2006**, *39*, 3978–3979.
- (67) Sulyok, G. A. G.; Gibson, C.; Goodman, S. L.; Hölzemann, G.; Wiesner, M.; Kessler, H. Solid-phase synthesis of a nonpeptide RGD mimetic library: new selective $\alpha_v\beta_3$ integrin antagonists. *J. Med. Chem.* **2001**, *44*, 1938–1950.
- (68) Porté-Durrieu, M. C.; Guillemot, F.; Pallu, S.; Labrugère, C.; Brouillaud, B.; Bareille, R.; Amédée, J.; Barthe, N.; Dard, M.; Baquey, Ch. Cyclo-(DfKRG) peptide grafting onto Ti-6Al-4V: physical characterization and interest towards human osteoprogenitor cells adhesion. *Biomaterials* **2004**, *25*, 4837–4846.
- (69) Pallu, S.; Bourget, C.; Bareille, R.; Labrugère, C.; Dard, M.; Sewing, A.; Jonczyk, A.; Vernizeau, M.; Durrieu, M. C.; Amédée-Vilamitjana, J. The effect of cyclo-DfKRG peptide immobilization on titanium on the adhesion and differentiation of human osteoprogenitor cells. *Biomaterials* **2005**, *26*, 6932–6940.
- (70) Landegren, U. Measurement of cell numbers by means of the endogenous enzyme hexosaminidase. Applications to detection of lymphokines and cell surface antigens. *J. Immunol. Methods* **1984**, *67*, 379–388.
- (71) Pfaff, M.; Tangemann, K.; Müller, B.; Gurrath, M.; Müller, G.; Kessler, H.; Timpl, R.; Engel, J. Selective recognition of cyclic RGD peptides of NMR defined conformation by $\alpha_{11b}\beta_3$, $\alpha_v\beta_3$, and $\alpha_5\beta_1$ integrins. *J. Biol. Chem.* **1994**, *269*, 20233–20238.
- (72) Xiong, J.-P.; Stehle, T.; Zhang, R.; Joachimiak, A.; Frech, M.; Goodman, S. L.; Arnaout, M. Crystal structure of the extracellular segment of integrin $\alpha_v\beta_3$ in complex with an Arg-Gly-Asp ligand. *Science* **2002**, *296*, 151–155.
- (73) Moitessier, N.; Henry, C.; Maigret, B.; Chapleur, Y. Combining pharmacophore search, automated docking, and molecular dynamics simulations as a novel strategy for flexible docking. Proof of concept: docking of arginine-glycine-aspartic acid-like compounds into the $\alpha_v\beta_3$ binding site. *J. Med. Chem.* **2004**, *47*, 4178–4187.
- (74) Manzoni, L.; Bassanini, M.; Belvisi, L.; Motto, I.; Scolastico, C.; Castorina, M.; Pisano, C. Nonpeptide integrin antagonists: RGD mimetics incorporating substituted azabicycloalkanes as amino acid replacements. *Eur. J. Org. Chem.* **2007**, 1309–1317.
- (75) Zanardi, F.; Burreddu, P.; Rassu, G.; Auzzas, L.; Battistini, L.; Curti, C.; Sartori, A.; Nicastro, G.; Menchi, G.; Cini, N.; Bottonocetti, A.; Raspanti, S.; Casiraghi, G. Discovery of subnanomolar arginine-glycine-aspartate-based $\alpha_v\beta_3/\alpha_v\beta_5$ integrin binders embedding 4-aminoproline residues. *J. Med. Chem.* **2008**, *51*, 1771–1782.
- (76) Momtaz, M.; Dewez, J.-L.; Marchand-Brynaert, J. Chemical reactivity assay and surface characterization of a poly(vinylidene fluoride) microfiltration membrane (Durapore DVPP). *J. Membr. Sci.* **2005**, *250*, 29–37.
- (77) Chollet, C.; Chanseau, C.; Remy, M.; Guignandon, A.; Bareille, R.; Labrugère, C.; Bordenave, L.; Durrieu, M.-C. The effect of RGD density on osteoblast and endothelial cell behavior on RGD-grafted polyethylene terephthalate surfaces. *Biomaterials* **2009**, *30*, 711–720.
- (78) Hartman, G. D.; Egbertson, M. S.; Halczenko, W.; Laswell, W. L.; Duggan, M. E.; Smith, R. L.; Naylor, A. M.; Manno, P. D.; Lynch, R. J.; Zhang, G.; Chang, C. T.-C.; Gould, R. J. Non-peptide fibrinogen receptor antagonists. 1. Discovery and design of exosite inhibitors. *J. Med. Chem.* **1992**, *35*, 4640–4642.
- (79) Owen, R. M.; Carlson, C. B.; Xu, J.; Mowery, P.; Fasella, E.; Kiessling, L. L. Bifunctional ligands that target cells displaying the $\alpha_v\beta_3$ integrin. *ChemBioChem* **2007**, *8*, 68–82.
- (80) Carlson, C. B.; Mowery, P.; Owen, R. M.; Dykhuizen, E. C.; Kiessling, L. L. Selective tumor cell targeting using low-affinity, multivalent interactions. *ACS Chem. Biol.* **2007**, *2*, 119–127.
- (81) Dijkgraaf, I.; Kruijtzter, J. A. W.; Frielink, C.; Soede, A. C.; Hilbers, H. W.; Oyen, W. J. G.; Corstens, F. H. M.; Liskamp, R. M. J.; Boerman, O. C. Synthesis and biological evaluation of potent $\alpha_v\beta_3$ integrin receptor antagonists. *Nucl. Med. Biol.* **2006**, *33*, 953–961.
- (82) Müller, B.; Zerwes, H. G.; Tangemann, K.; Peter, J.; Engel, J. 2-Step binding mechanism of fibrinogen to $\alpha_{11b}\beta_3$ integrin reconstituted into planar lipid bilayers. *J. Biol. Chem.* **1993**, *268*, 6800–6808.
- (83) Vilamitjana-Amédée, J.; Bareille, R.; Rouais, F.; Caplan, A. E.; Harmand, M. F. Human bone marrow stromal cells expressing osteoblastic phenotype in vitro. *Cell. Dev. Biol.* **1993**, *29*, 699–707.
- (84) Villars, F.; Guillotin, B.; Amédée, T.; Dutoya, S.; Bordenave, L.; Bareille, R.; Amédée, J. Effect of HUVEC on human osteoprogenitor cell differentiation needs heterotypic gap junction communication. *Am. J. Physiol. Cell. Physiol.* **2002**, *282*, C775–C785.
- (85) Hariharan, P. C.; Pople, J. A. The influence of polarization functions on molecular hydrogenation energies. *Theor. Chim. Acta* **1973**, *28*, 213–217.
- (86) Dive, G.; Dehareng, D.; Ghuysen, J. M. Energy analysis of small to medium sized H-bonded complexes. *Theor. Chim. Acta* **1993**, *85*, 409–421.
- (87) Frisch, M. J.; Trucks, G. W.; Schlegel, H. B.; Scuseria, G. E.; Robb, M. A.; Cheeseman, J. R.; Montgomery, J. A.; Jr.; Vreven, T.; Kudin, K. N.; Burant, J. C.; Millam, J. M.; Iyengar, S. S.; Tomasi, J.; Barone, V.; Mennucci, B.; Cossi, M.; Scalmani, G.; Rega, N.; Petersson, G. A.; Nakatsuji, H.; Hada, M.; Ehara, M.; Toyota, K.; Fukuda, R.; Hasegawa, J.; Ishida, M.; Nakajima, T.; Honda, Y.; Kitao, O.; Nakai, H.; Klene, M.; Li, X.; Knox, J. E.; Hratchian, H. P.; Cross, J. B.; Adamo, C.; Jaramillo, J.; Gomperts, R.; Stratmann, R. E.; Yazyev, O.; Austin, A. J.; Cammi, R.; Pomelli, C.; Ochterski, J. W.; Ayala, P. Y.; Morokuma, K.; Voth, G. A.; Salvador, P.; Dannenberg, J. J.; Zakrzewski, V. G.; Dapprich, S.; Daniels, A. D.; Strain, M. C.; Farkas, O.; Malick, D. K.; Rabuck, A. D.; Raghavachari, K.; Foresman, J. B.; Ortiz, J. V.; Cui, Q.; Baboul, A. G.; Clifford, S.; Cioslowski, J.; Stefanov, B. B.; Liu, G.; Liashenko, A.; Piskorz, P.; Komaromi, I.; Martin, R. L.; Fox, D. J.; Keith, T.; Al-Laham, M. A.; Peng, C. Y.; Nanayakkara, A.; Challacombe, M.; Gill, P. M. W.; Johnson, B.; Chen, W.; Wong, M. W.; Gonzalez, C.; Pople, J. A. *Gaussian 03, revision C.02*; Gaussian, Inc.: Wallingford, CT, 2004.
- (88) Pourcelle, V.; Devouge, S.; Garinot, M.; Préat, V.; Marchand-Brynaert, J. PCL-PEG-based nanoparticles grafted with GRGDS peptide: preparation and surface analysis by XPS. *Biomacromolecules* **2007**, *8*, 3977–3983.
- (89) Golledge, J.; Tumer, R. J.; Harley, S. L.; Springall, D. R.; Powell, J. T. Development of an in vitro model to study the response of saphenous vein endothelium to pulsatile arterial flow and circumferential deformation. *Eur. J. Vasc. Endovasc. Surg.* **1997**, *13*, 605–612.